https://ntrs.nasa.gov/search.jsp?R=19930085812 2020-06-17T16:03:53+00:00Z

Copy No. 184

[redacted]

RM No. L6L27

NACA

RESEARCH MEMORANDUM

ENGINEERING DEPT. LIBRARY
CHANCE VOUGHT AIRCRAFT
STRATFORD, CONN.

EFFECTS OF A FUSELAGE AND VARIOUS HIGH-LIFT AND STALL-CONTROL FLAPS ON AERODYNAMIC CHARACTERISTICS IN PITCH OF AN NACA 64-SERIES 40° SWEPT-BACK WING

By

D. William Conner and Robert H. Neely

Langley Memorial Aeronautical Laboratory
Langley Field, Va.

CLASSIFIED D[redacted]NT

This document conta[redacted]ified information affecting the Natio[redacted]nse of the United States within the m[redacted]f the Espionage Act, USC 50:31 and 3[redacted] transmission or the revelation of its[redacted]s in any manner to an unauthorized p[redacted]s prohibited by law. Information [redacted]ssified may be imparted only to pe[redacted]n the military and naval services [redacted]United States, appropriate civilian [redacted] and employees of the Federal Governm[redacted]ho have a legitimate interest therein[redacted]o United States citizens of known loyal[redacted]iscretion who of necessity must be info[redacted]ereof.

NATIONAL ADVISORY COMMITTEE FOR AERONAUTICS

WASHINGTON

May 26, 1947

[redacted]

RM L6L27

NATIONAL ADVISORY COMMITTEE FOR AERONAUTICS

RESEARCH MEMORANDUM

EFFECTS OF A FUSELAGE AND VARIOUS HIGH-LIFT AND STALL-CONTROL FLAPS ON AERODYNAMIC CHARACTERISTICS IN PITCH OF AN NACA 64-SERIES 40° SWEPT-BACK WING

By D. William Conner and Robert H. Neely

SUMMARY

Wind-tunnel tests were made to determine the low-speed lift, drag, and pitching-moment characteristics of a 40° swept-back wing tested with high-lift and stall-control flaps and tested with a fuselage having a fineness ratio of 10.2 to 1. The wing had an aspect ratio of 4, taper ratio of 0.625, and NACA 64_1-112 sections perpendicular to the quarter-chord line. High-lift and stall-control flaps tested on the wing without the fuselage at Reynolds numbers of 3,000,000 and 6,800,000 included semispan normal split flaps, semispan split flaps hinged at the wing trailing edge, constant-chord leading-edge flaps, and upper-surface flaps. Low-, middle-, and high-wing-fuselage combinations were tested at Reynolds numbers of 3,000,000 and 8,100,000.

At a Reynolds number of 6,800,000, the maximum lift coefficients of the wing with no flaps, with semispan normal split flaps and with semispan split flaps hinged at the trailing edge of the wing were 1.11, 1.32, and 1.40, respectively. The corresponding values obtained by the addition of 0.725-span outboard leading-edge flaps were 1.29, 1.55, and 1.73. The leading-edge flaps tested eliminated both the tip stalling and longitudinal instability that were obtained at maximum lift with the plain wing. The outboard upper-surface flaps, as tested, caused a large rearward shift in aerodynamic-center location but were unsatisfactory because of large reductions in lift, large changes in trim, large increases in drag, and no improvement of the wing-tip stalling characteristics.

At both low and high Reynolds numbers the fuselage in the low-, middle-, and high-wing positions had little effect on lift and stalling, and at low angles of attack, moved the aerodynamic center ahead as much as 3 percent of the mean aerodynamic chord. Near maximum lift and at a Reynolds number of 8,100,000, the forward shift of the aerodynamic center with flaps off varied from about 3 percent for the low-wing position to 11 percent for the high-wing position.

[redacted]

In the high-lift range, the increase in drag coefficient caused by adding the fuselage in any position to the unflapped wing amounted to only 0.0050.

INTRODUCTION

The low-speed aerodynamic characteristics of a 40° swept-back wing of aspect ratio 4, taper ratio 0.625, and NACA 64_1-112 sections were reported in reference 1. This wing, like many swept-back wings, was longitudinally unstable at the stall because of wing-tip stalling and had relatively low values of maximum lift coefficient even with semispan split flaps. In an attempt to alleviate tip stalling and/or increase the maximum lift, tests have been made of the wing equipped with leading-edge flaps, outboard upper-surface flaps, and split flaps hinged at the wing trailing edge. These tests were made at Reynolds number values of 3,040,000 and 6,840,000.

In order to investigate the effect of a fuselage on the aerodynamic characteristics of the wing, tests have also been made of this wing with a fuselage in low, middle, and high positions. The tests were made to determine the characteristics in pitch at Reynolds number values of 3,040,000 and 8,090,000.

COEFFICIENTS AND SYMBOLS

All data are referred to the wind axes. The dimensions used in computing all coefficients are those for the basic wing.

C_L lift coefficient (L/qS)

$\Delta C_{L_{max}}$ increment in maximum lift coefficient

C_D drag coefficient (D/qS)

C_m pitching-moment coefficient $(M/qS\bar{c})$

C_l rolling-moment coefficient (L'/qSb)

R Reynolds number $(\rho V\bar{c}/\mu)$

M Mach number (V/a)

α angle of attack of wing chord line

[redacted]

where

L lift

D drag

M pitching moment (about quarter chord of mean aerodynamic chord)

L' rolling moment

S wing area

b wing span

$\bar{c}$ mean aerodynamic chord measured parallel to the plane of symmetry $\left(\frac{2}{S}\int_0^{b/2} c^2\,dy\right)$

$\bar{x}$ distance from the leading edge of the root chord (at the plane of symmetry) to the quarter-chord point of the mean aerodynamic chord $\left(\frac{2}{S}\int_0^{b/2} cx\,dy\right)$

x longitudinal distance from the leading edge of root chord to quarter-chord point of each section parallel to plane of symmetry

c local chord measured parallel to the plane of symmetry

y spanwise coordinate

q free-stream dynamic pressure $\left(\frac{1}{2}\rho V^2\right)$

V free-stream velocity

ρ mass density of air, slugs per cubic foot

μ coefficient of viscosity

a velocity of sound

MODEL

The plan and side views of the wing and fuselage are shown in figure 1. The angle of sweep of the quarter-chord line of the wing is 40° and the wing sections perpendicular to the quarter-chord line are NACA 64_1-112 sections. The quarter-chord line of each wing panel is herein defined as the quarter-chord line of a straight panel which has been rotated 40° about the quarter-chord point of its root chord. The aspect ratio is 4.01 and the taper ratio is 0.625. The wing has no geometric dihedral or twist.

The installation of the various high-lift and stall-control flaps on the wing are shown in figure 2. The normal split flaps (fig. 2(a)) extend over the inboard 50 percent of the wing span. For the fuselage-on tests a section of the flap (12.3 percent of the wing span) was removed at the wing center. The flap chord is 20 percent of the wing chord normal to the quarter-chord line, and the flap deflection with respect to the 80-percent wing-chord (hinge) line is 60°, measured between the wing lower surface and the flap. The same flaps were tested in an extended arrangement shown in figure 2(b) where the hinge line was moved to the wing trailing edge. The deflection duplicated that of the normal split flaps. The flaps were fabricated of sheet metal.

The dimensions of the leading-edge flap are given in figure 2(c). Sheet metal was curved, welded to a $\frac{1}{2}$-inch-diameter steel tube at the leading edge, then faired to give the desired contour. The radius of the tube is, on the average, equal to the leading-edge radius of the airfoil. The flap has a constant chord and was faired smoothly into the upper wing surface by means of modeling clay. (See fig. 3.) As measured in a plane perpendicular to the wing quarter-chord line, a line connecting the leading edge of the wing with the leading edge of the flap has a 50° incidence with the wing chord. The length of the line is 3.19 inches, which in terms of the local wing chord, corresponds to 10 percent at the inboard end of the flap and 14.3 percent at the outboard end. The complete flap span is 72.5 percent of the wing semispan. The inboard end is located at 25 percent of the wing semispan and the flap extends to 97.5 percent wing semispan (where the wing tip starts to round off). Some tests were made with an inboard section of the flap removed to give a flap span of 57.5 percent of the wing semispan. Figure 3 shows the flap mounted on the wing.

The 20-percent-chord sheet-metal upper-surface flap, shown in figure 2(d), deflects up and back from the wing trailing edge and was tested only in conjunction with the extended split flaps. The flap deflection measured in a plane perpendicular to the wing quarter-chord line is 60° with respect to a plane tangent to the wing-upper-surface 80 percent-chord station.

The fuselage has a fineness ratio of 10.2 to 1 and a circular cross section, the maximum diameter being 40 percent of the root chord (fig. 1). The section of the fuselage intersected by the wing has a constant diameter. Percentages of this diameter are used to fix the three vertical locations of the wing root quarter-chord point with respect to the fuselage center line. They are: 37.5 percent below, zero percent, and 37.5 percent above. In each of these three positions tested, the wing chord plane has a positive incidence of 2° with respect to the fuselage center line. No fillets were used at the wing-fuselage juncture. The high-wing fuselage combination mounted for testing is shown in figure 4. Both wing and fuselage were constructed of laminated mahogany, then lacquered and sanded to obtain aerodynamically smooth surfaces.

TESTS

Tests were made in the Langly 19-foot pressure tunnel with the wing mounted on a two-support system as shown in figure 4. Lift, drag, pitching moment, and rolling moment were measured for values of Reynolds number and Mach number as follows:

R	M
3,040,000	0.069
6,840,000	0.156
8,090,000	0.190

The values of Reynolds number were maintained to within ±40,000.

Tests of the various high-lift and stall-control flaps were made with the wing alone at Reynolds number values of 3,040,00 and 6,840,000. All fuselage-on tests were made with and without split flaps at Reynolds number values of 3,040,000 and 8,090,000. Only one fuselage-off, flaps-on test was made which compared directly with the fuselage-on, flaps-on condition (inboard section of flaps removed). The Reynolds number value of that test was 6,840,000 and the aerodynamic results are believed to have practically the same characteristics as those for a higher value of Reynolds number.

(See reference 1.) Stall characteristics were studied by means of tufts attached to the wing upper surface beginning at 20 percent of the wing chord.

RESULTS AND DISCUSSION

The corrections applied to the data of reference 1, and discussed therein, have been applied to all data included in this report.

The lift, drag, and pitching-moment characteristics of the wing equipped with various high-lift and stall-control flaps are presented in figures 5 through 9. In a few instances the rolling-moment characteristics near maximum lift are included. The locations of the aerodynamic centers for some of these configurations are given in figure 10. Some of the more important characteristics at a Reynolds number of 6,840,000 are given in table I for comparing the effects of the various flaps. Flow conditions over the plain wing and the wing equipped with the various flaps are shown in figures 11 and 12. The lift, drag, and pitching-moment characteristics for the various wing-fuselage combinations are presented in figures 13 through 16. The pitching-moment coefficients are presented not only as a function of lift coefficients but also, at high angles of attack, as a function of angle of attack. The location of the aerodynamic centers for these fuselage combinations at $R = 8,090,000$ are given in figure 17. Flow conditions over the wing with fuselage are shown in figure 18.

High-Lift and Stall-Control Flaps

The discussion given in the following paragraphs on the effects of the various flaps is based upon data obtained at $R = 6,840,000$ unless otherwise noted.

Split flaps.- The addition of semispan normal split flaps increased $C_{L_{max}}$ from 1.11 to 1.32 and the pitching-moment curve was shifted negatively ranging from 0.025 to 0.040, with no change in the unstable break at the stall. (See fig. 5.) As in the case of the plain wing an abrupt stall occurred on the outer portion of the wing (fig. 11) and, as can be seen from the stall diagrams and rolling-moment data of figure 5, the right-wing panel stalled first. This asymmetry was attributed to small differences in the wing-surface contours. Extending the split flaps until the hinge line was on the trailing edge increased the untrimmed value of $C_{L_{max}}$ from

1.32 to 1.40. The value of C_m was shifted negatively about 0.05 but an unstable change still occurred at the stall. Decreasing the Reynolds number from 6,840,000 to 3,040,000 caused a stable negative break in pitching moment at the stall. (See figs. 5 and 8(a).) Flow studies showed that the initial stall extended inboard from the wing tip about $0.25\frac{b}{2}$ at $R = 6,840,000$ and $0.50\frac{b}{2}$ at $R = 3,040,000$.

Leading-edge flaps.- The addition of leading-edge flaps extended the lift curve so that maximum lift occurred at a much higher angle of attack than was observed for the plain wing. (See fig. 6.) The $0.575\frac{b}{2}$-span and $0.725\frac{b}{2}$-span leading-edge flaps gave increases in $C_{L_{max}}$ equal to 0.12 and 0.18, respectively, but the largest gains resulted when the $0.725\frac{b}{2}$-span flaps were tested in conjunction with the split flaps. With normal split flaps $C_{L_{max}}$ increased to 1.55, equal to a $\Delta C_{L_{max}}$ of 0.44 above wing-alone test results or 0.23 above normal-split-flap test results. With extended split flaps $C_{L_{max}}$ increased to 1.73 equal to a $\Delta C_{L_{max}}$ of 0.62 above wing-alone test results or 0.33 above extended-split-flap test results. In tests with extended split flaps, where the leading-edge-flap span was reduced from $0.725\frac{b}{2}$ to $0.575\frac{b}{2}$, $C_{L_{max}}$ decreased from 1.73 to 1.52. The value of $\Delta C_{L_{max}}$ was only 0.41 above wing-alone test results. This value was exactly the sum of the $C_{L_{max}}$-increments obtained when each flap was tested separately. In connection with this reduction in lift with flap span it is interesting to note that both the angle of attack at $C_{L_{max}}$ and the amount of wing area stalled at $C_{L_{max}}$ were considerably less for the shorter-span flap configuration than for the longer-span flap configuration. (See figs. 12(b) and 12(c).)

The addition of leading-edge flaps caused no large displacements in pitching moment at all values of C_L up to within 0.1 of $C_{L_{max}}$. In this same range, a slight destabilizing effect was obtained. As can be seen from figure 10, large rearward shifts in the aerodynamic center occurred just below maximum lift and, at the stall, the pitch characteristics were considered satisfactory. These characteristics, differing radically from the results of the wing tested without leading-edge flaps, can be explained by the stall progressions shown in figures 11 and 12. Without leading-edge flaps, a sudden stall occurred over the outer half of the wing (fig. 11) causing a forward, unstable change in aerodynamic center. With leading-edge flaps, the first rough flow was noticed at moderate values of lift coefficient immediately behind the inboard ends of the leading-edge flaps. As the angle of attack was increased, these areas of rough flow gradually fanned out rearward and became stalled until at maximum lift the central sections of the wing were almost completely stalled with only the wing tips remaining unstalled. This type of stall progression shifted the aerodynamic center rearward (figs. 12(a) and 12(b)) and would also be considered favorable in retaining lateral control.

The ratio of drag to the lift is a measure of the glide-path angle and sinking speed. With leading-edge flaps on, this ratio at maximum lift was from 40 to 90 percent higher than the ratio for the wing with split flaps. (See table I.)

Decreasing the Reynolds number value from 6,840,000 to 3,040,000 caused only small changes in the aerodynamic characteristics when the leading-edge flaps were on, in contrast to the large changes obtained with leading-edge flaps off. Unpresented aerodynamic data were obtained at $R = 6,840,000$ with leading-edge and split flaps on to determine the effect of a small discontinuity at the leading-edge flap-wing juncture. This discontinuity was effected by removing the modeling clay fairing the juncture but leaving the gap sealed. There were no aerodynamic changes measured.

In general, the leading-edge flaps eliminated both the tip stalling and longitudinal instability that were obtained at maximum lift with the plain wing and, in combination with split flaps, gave substantial increases in the value of maximum lift coefficient. The larger drag coefficients, obtained near maximum lift, however, might limit the lift coefficient that could be satisfactorily used.

Upper-surface flaps.- Upper-surface flaps, which were tested in conjunction with extended flaps, reduced C_L by 0.3 and displaced C_m by 0.20 at low angles of attack. (See fig. 9.) As the angle of attack increased there was a decrease in both the lift decrement and the pitching-moment increment due to the flaps. As a result, the pitching-moment variation was stable. At $R = 6,840,000$, the sudden stall was of a severe enough nature to endanger the model structure thus prohibiting the taking of force measurements beyond maximum lift. The stall pattern was observed and is shown in figure 12(d). The stalled regions blanketed the wing tips but not the wing center sections. The upper-surface flaps caused large increases in drag. Because of the large aerodynamic changes these particular upper-surface flaps are not considered satisfactory. It is possible that upper-surface flaps of a different design might effect satisfactory pitch characteristics at the stall without too large sacrifices in lift and drag.

Wing-Fuselage Combinations

The presence of the fuselage on the wing with and without normal split flaps had little effect on the lift characteristics regardless of position, $dC_L/d\alpha$ was increased up to .003 and $C_{L_{\alpha=0}}$ and $C_{L_{max}}$ were within 0.03 of the wing-alone values (figs. 13 and 14). In the basic fuselage-off tests, with normal split flaps on, the inboard section of the flaps were removed causing a decrease in $C_{L_{\alpha=0}}$ of 0.10 and $C_{L_{max}}$ of 0.04.

At low lifts the pitching-moment curves were displaced by increments in C_m of -0.008 to -0.015 with flaps off and -0.018 to -0.024 with flaps on. Also it is seen from figure 17 that the aerodynamic center moved forward 1.8 percent and 2.8 percent of the mean aerodynamic chord, flaps off and flaps on, respectively. The most significant influence on any of the characteristics was the effect of fuselage position on the forward movement of the aerodynamic center near maximum lift. With flaps off at $C_L = 1.05$, this shift varied from 3 percent of the mean aerodynamic chord for the low-wing position to 11 percent for the high-wing position. With flaps on at $C_L = 1.2$, this shift with fuselage position was from 1.5 to 4 percent, low-wing to high-wing position.

As can be seen from figures 11 and 18, the stall progression was not altered to any great degree. A small region of rough flow developed at high lifts on the wing near the fuselage juncture for the low-wing flaps-off combination.

At zero lift, flaps off, C_D increased by amounts ranging from 0.0030 (midwing) to 0.0045 (high wing). At $C_L = 1$, the increase in C_D equaled 0.0050 for all fuselage positions. With flaps on, the additional drag contributed by the flap cut-out varied with fuselage position and disguised any fuselage drag increases.

The large forward movement of the aerodynamic center obtained just below the moment-curve break with the high-wing configuration at $R = 8,090,000$ was not obtained at $R = 3,040,000$, but a somewhat similar shift was obtained at a lower lift coefficient. Except for this difference the effects of the fuselage were about the same at $R = 3,040,000$ and $8,090,000$.

In general, the fuselage in low-, middle-, and high-wing positions had no large adverse effects on maximum lift, and drag like those resulting from an interference burble as reported in reference 2. Also in reference 2, it is pointed out that "in the region of the maximum diameter of the fuselage, large changes in the fore-and-aft position of the wing apparently have little effect." Because of the geometry of this fuselage, moderate shifts, fore and aft, of the wing location should cause no large aerodynamic changes (provided account is taken of the changed relative location of the fuselage aerodynamic center).

CONCLUSIONS

The main results for the investigation were as follows:

1. At a Reynolds number of 6,840,000, the maximum lift coefficients of the wing with no flaps, with semispan normal split flaps and semispan split flaps hinged at the trailing edge of the wing were 1.11, 1.32, and 1.40, respectively. The corresponding values obtained by the addition of 0.725-span outboard leading-edge flaps were 1.29, 1.55, and 1.73.

2. The leading-edge flaps tested eliminated both the tip stalling and longitudinal instability that were obtained at maximum lift with the plain wing.

3. The outboard upper-surface flaps, as tested, caused a large rearward shift in aerodynamic-center location but were unsatisfactory because of large reductions in lift, large changes in trim, large increases in drag, and no improvement of the wing-tip stalling characteristics.

4. At Reynolds numbers of 3,040,000 and 8,090,000 the fuselage in the low-, middle-, and high-wing positions had little effect on lift and stalling, and at low angles of attack, moved the aerodynamic center ahead as much as 3 percent of the mean aerodynamic chord. Near maximum lift and at a Reynolds number of 8,090,000, the forward shift of the aerodynamic center with flaps off varied from about

3 percent for the low-wing position to 11 percent for the high-wing position. In the high-lift range, the increase in drag coefficient caused by adding the fuselage in any position to the unflapped wing amounted to only 0.0050.

Langley Memorial Aeronautical Laboratory
National Advisory Committee for Aeronautics
Langley Field, Va.

REFERENCES

1. Neely, Robert H., and Conner, D. William: Aerodynamic Characteristics of a 42° Swept-Back Wing with Aspect Ratio 4 and NACA 64_1-112 Airfoil Sections at Reynolds Numbers from 1,700,000 to 9,500,000. NACA RM No. L7D14, 1947.

2. Jacobs, Eastman N., and Ward, Kenneth E.: Interference of Wing and Fuselage from Tests of 209 Combinations in the N.A.C.A. Variable-Density Tunnel. NACA Rep. No. 540, 1935.

TABLE I.- CHARACTERISTICS OF 40° SWEPT-BACK WING WITH VARIOUS HIGH-LIFT AND STALL-CONTROL FLAPS. $R = 6,840,000$

Modifications	$C_{L_{max}}$	$\Delta C_{L_{max}}$	C_m at $C_{L_{max}}$	Type of C_m-curve at stall	D/L at $C_{L_{max}}$	From figure
None (plain wing)	1.11	------	-0.010	Unstable	0.114	5
$0.50\frac{b}{2}$ normal split flaps	1.32	0.21	-.058	Unstable	.154	5
$0.50\frac{b}{2}$ extended split flaps	1.40	.29	-.105	Unstable	.156	5
$0.575\frac{b}{2}$ leading-edge flaps	1.23	.12	-.070	Stable	.293	6
$0.725\frac{b}{2}$ leading-edge flaps	1.29	.18	-.078	Stable	.276	6
$0.725\frac{b}{2}$ leading-edge flaps + $0.50\frac{b}{2}$ normal split flaps	1.55	.44	-.025	Stable	.239	7
$0.725\frac{b}{2}$ leading-edge flaps + $0.50\frac{b}{2}$ extended split flaps	1.73	.62	-.086	Stable	.260	8
$0.575\frac{b}{2}$ leading-edge flaps + $0.50\frac{b}{2}$ extended split flaps	1.52	.41	-.100	Stable	.224	8

NATIONAL ADVISORY
COMMITTEE FOR AERONAUTICS

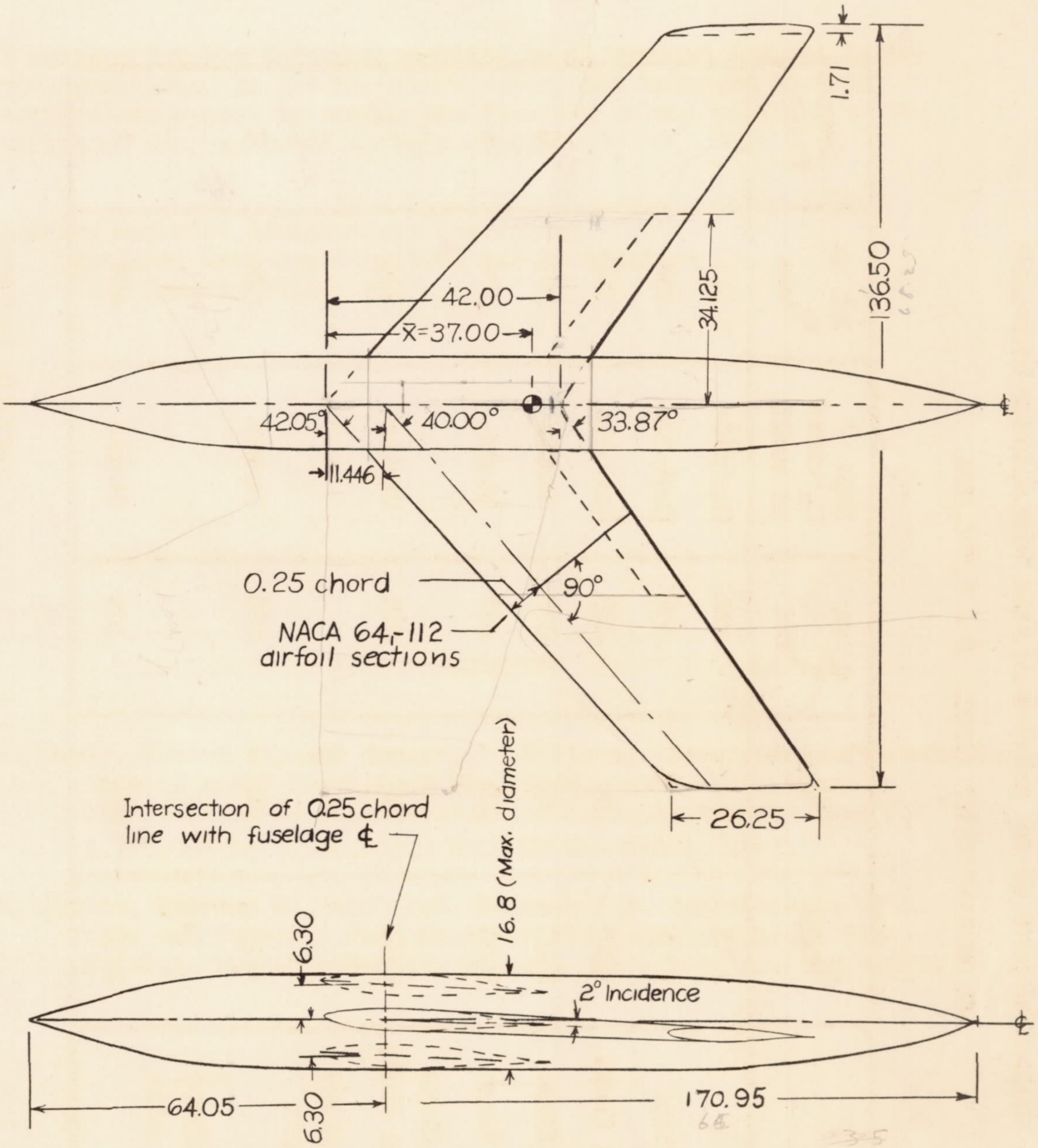

Fuselage Ordinates			
Distance behind fuselage nose	Fuselage diameter	Distance behind fuselage nose	Fuselage diameter
0	0.20	112.00	16.80
18.00	9.84	122.00	16.32
22.05	11.80	132.00	14.90
27.39	13.80	142.00	12.52
34.56	15.60	151.20	9.46
42.35	16.60	162.00	4.78
48.00	16.80	170.95	0

NATIONAL ADVISORY COMMITTEE FOR AERONAUTICS

Figure 1.- Geometry of 40° sweptback wing and fuselage. Aspect ratio = 4.01 ; wing area = 4643 sq in. ;M.A.C. =34.71in. (All dimensions in inches.)

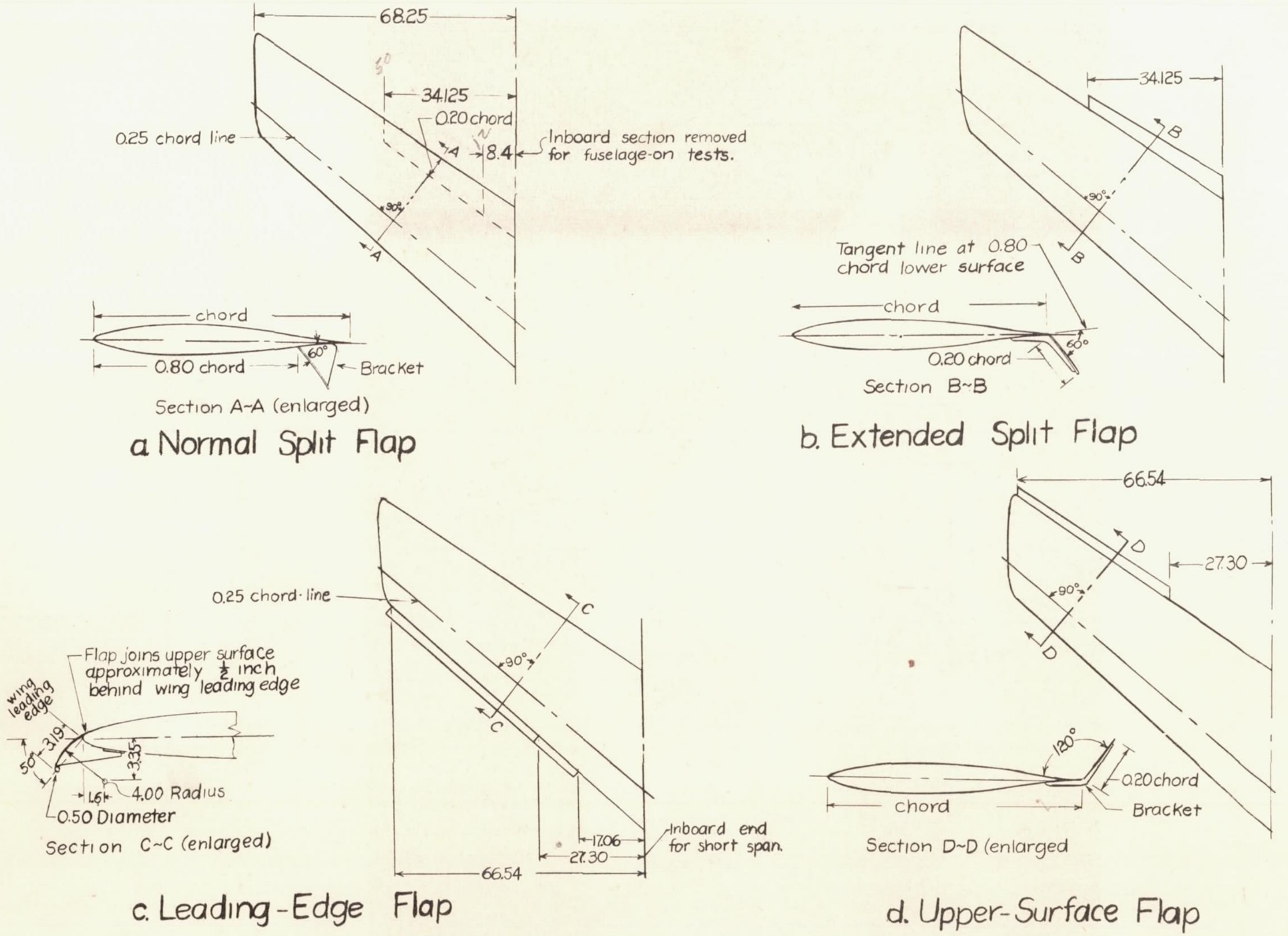

Figure 2.- Installation of high-lift and stall-control flaps on 40° sweptback wing. (All dimensions in inches.)

NATIONAL ADVISORY COMMITTEE FOR AERONAUTICS

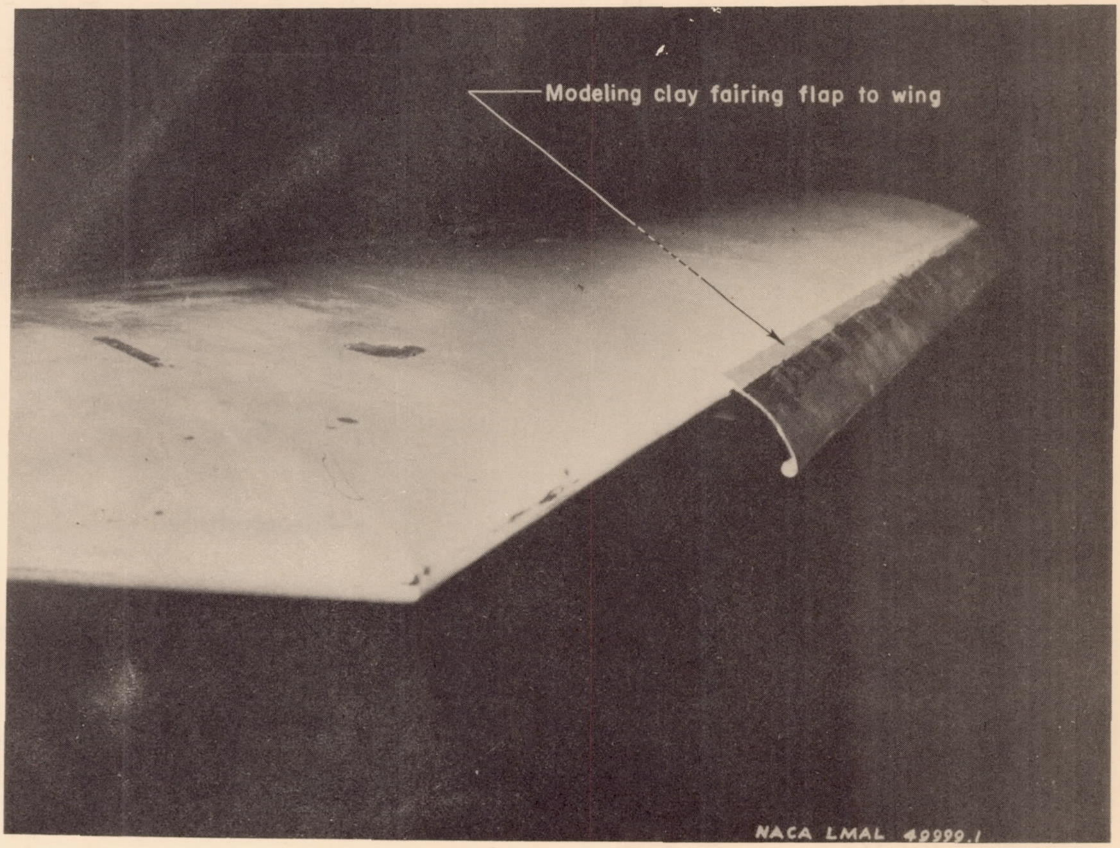

Figure 3.- Leading-edge flap mounted on 40° sweptback wing.

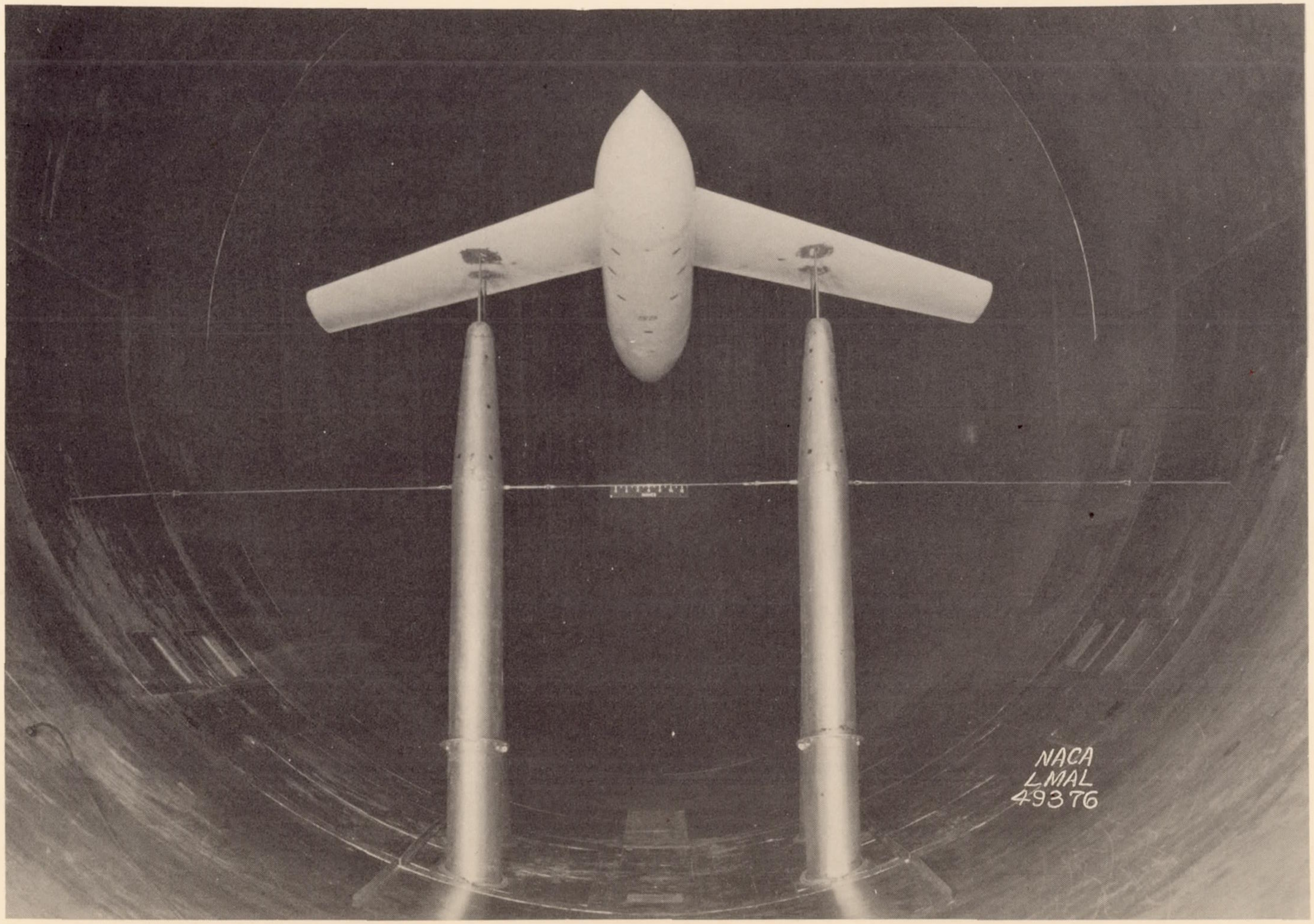

(a) Front view, high-wing fuselage combination.

Figure 4.- 40° sweptback wing mounted for testing in the Langley 19-foot pressure tunnel.

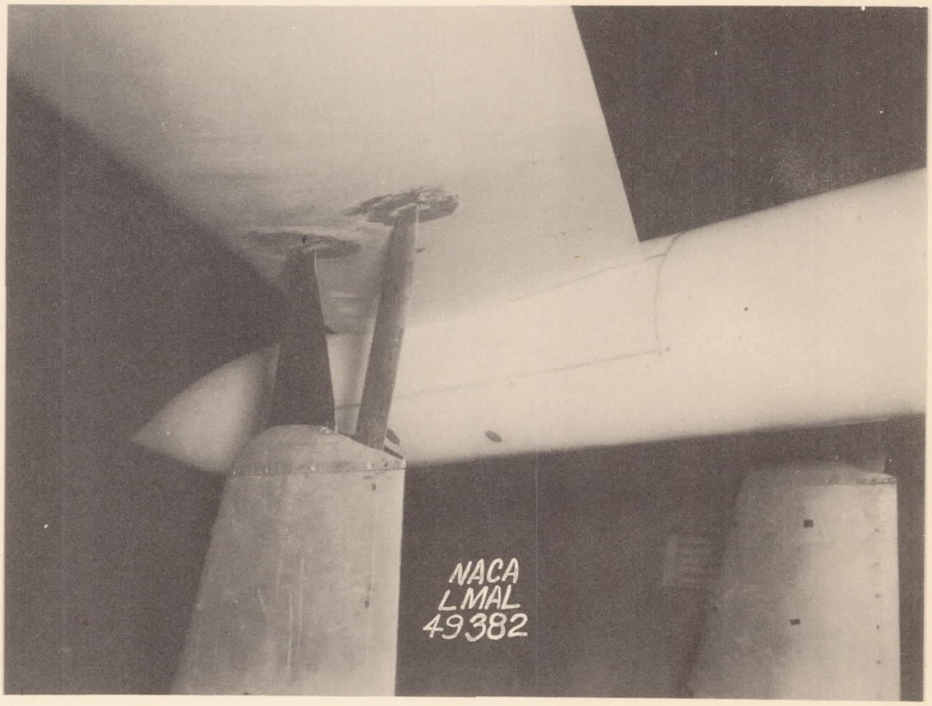

(b) Support details.

Figure 4.- Concluded.

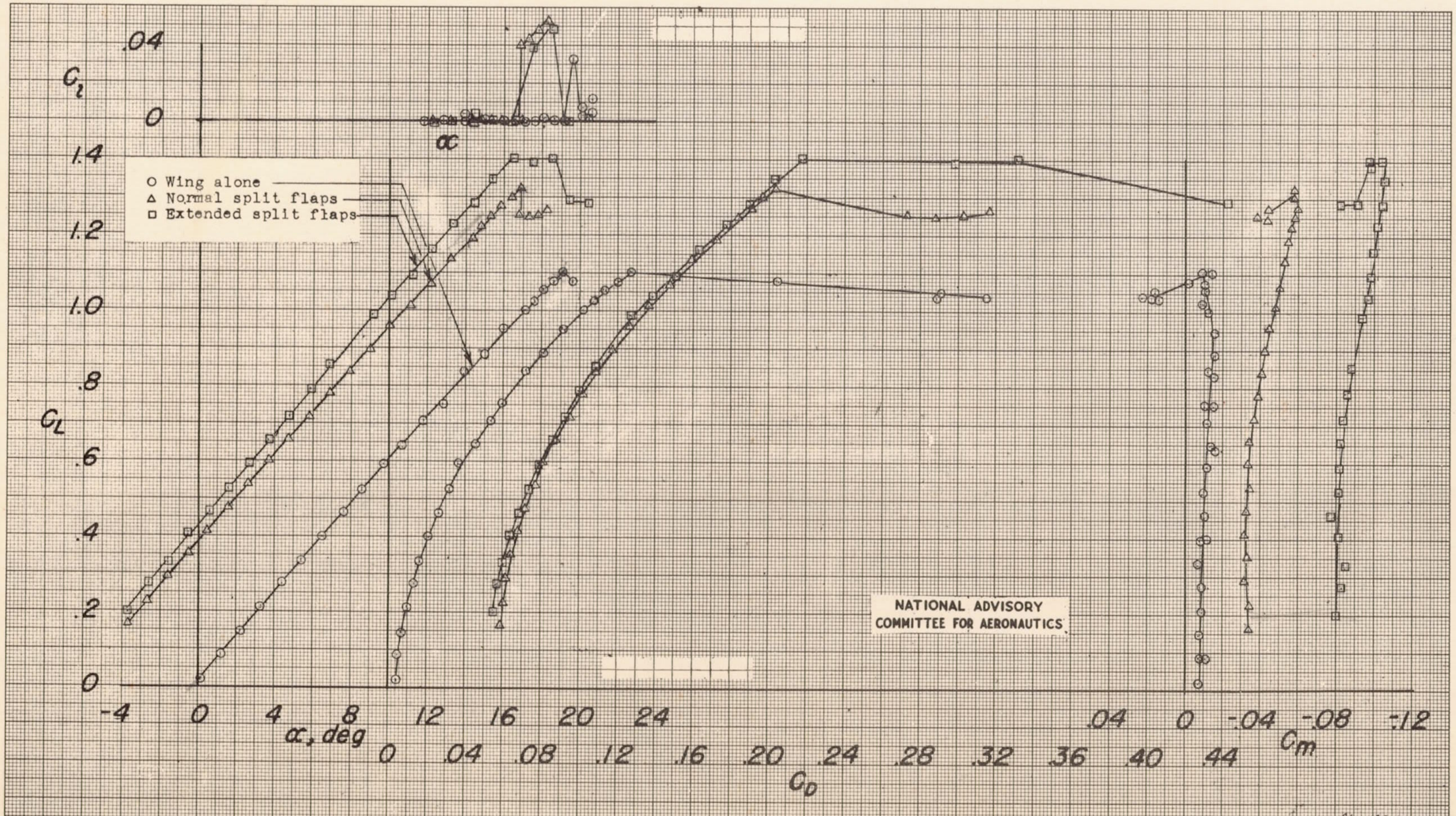

Figure 5.- Aerodynamic characteristics of a 40° sweptback wing with split flaps. R = 6,840,000.

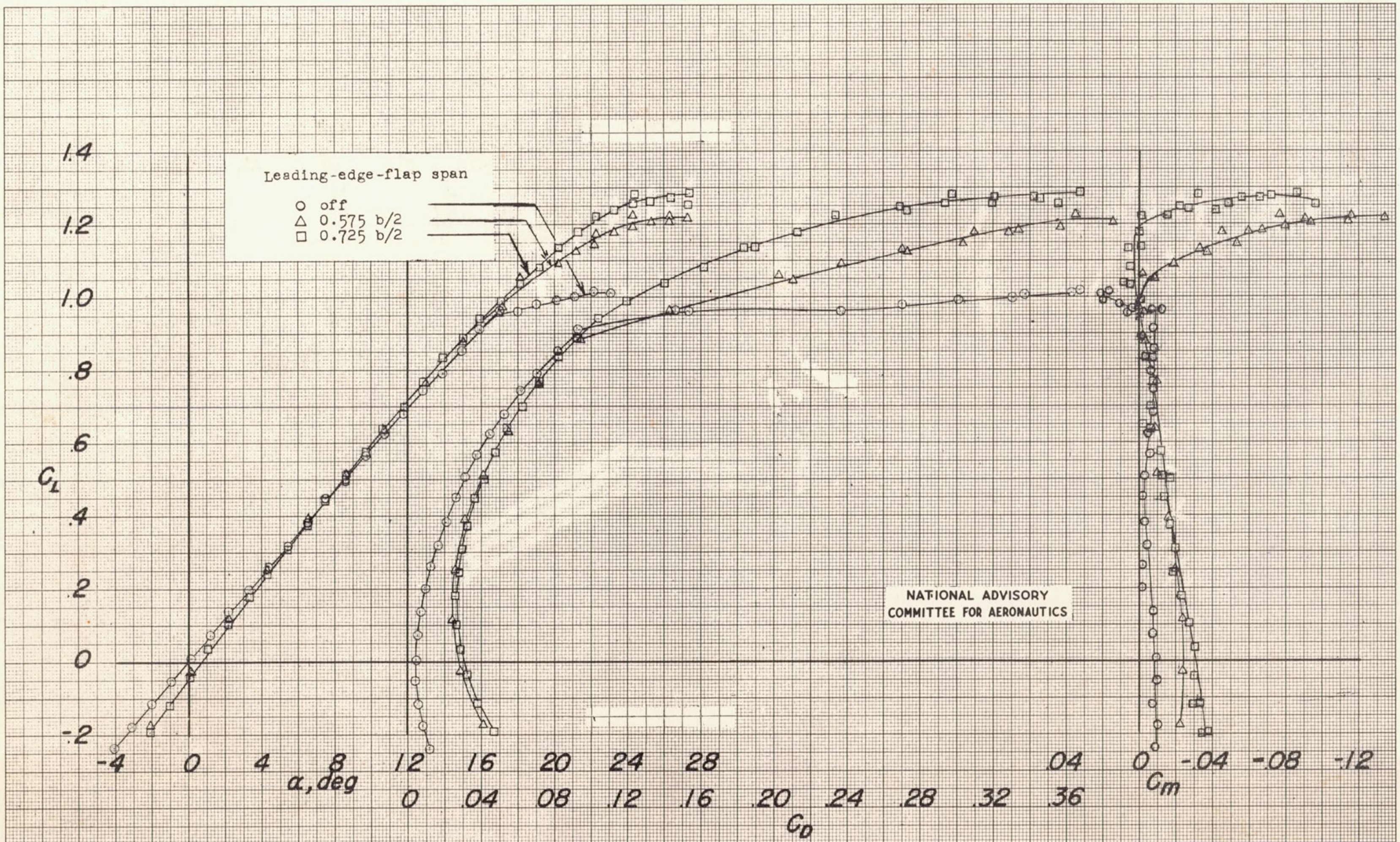

(a) R = 3,040,000.

Figure 6.- Aerodynamic characteristics of a 40° sweptback wing with and without leading-edge flaps. Trailing-edge flaps off.

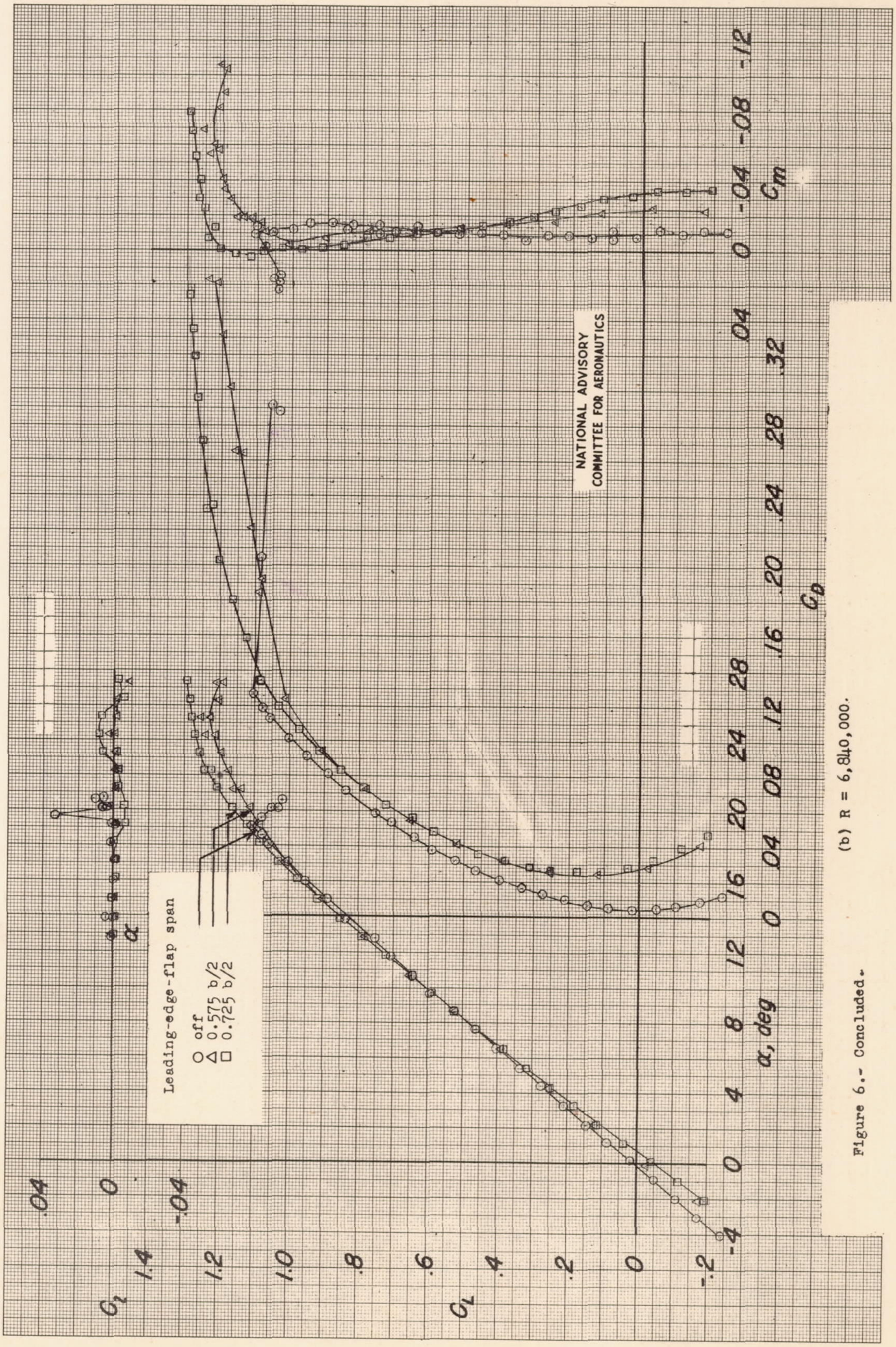

(b) R = 6,840,000.

Figure 6.- Concluded.

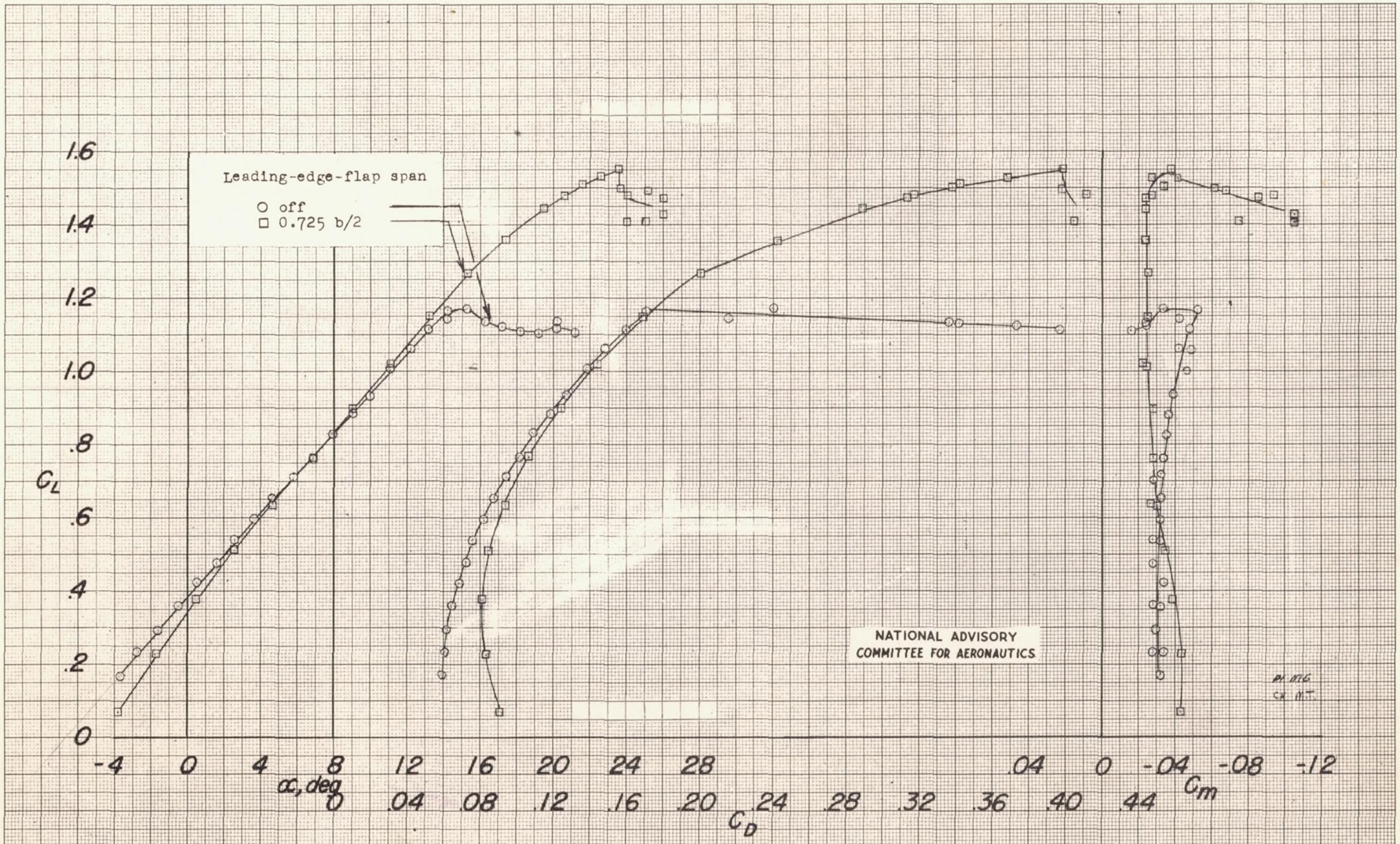

(a) R = 3,040,000.

Figure 7.- Aerodynamic characteristics of a 40° sweptback wing with and without leading-edge flaps. Normal split flaps on.

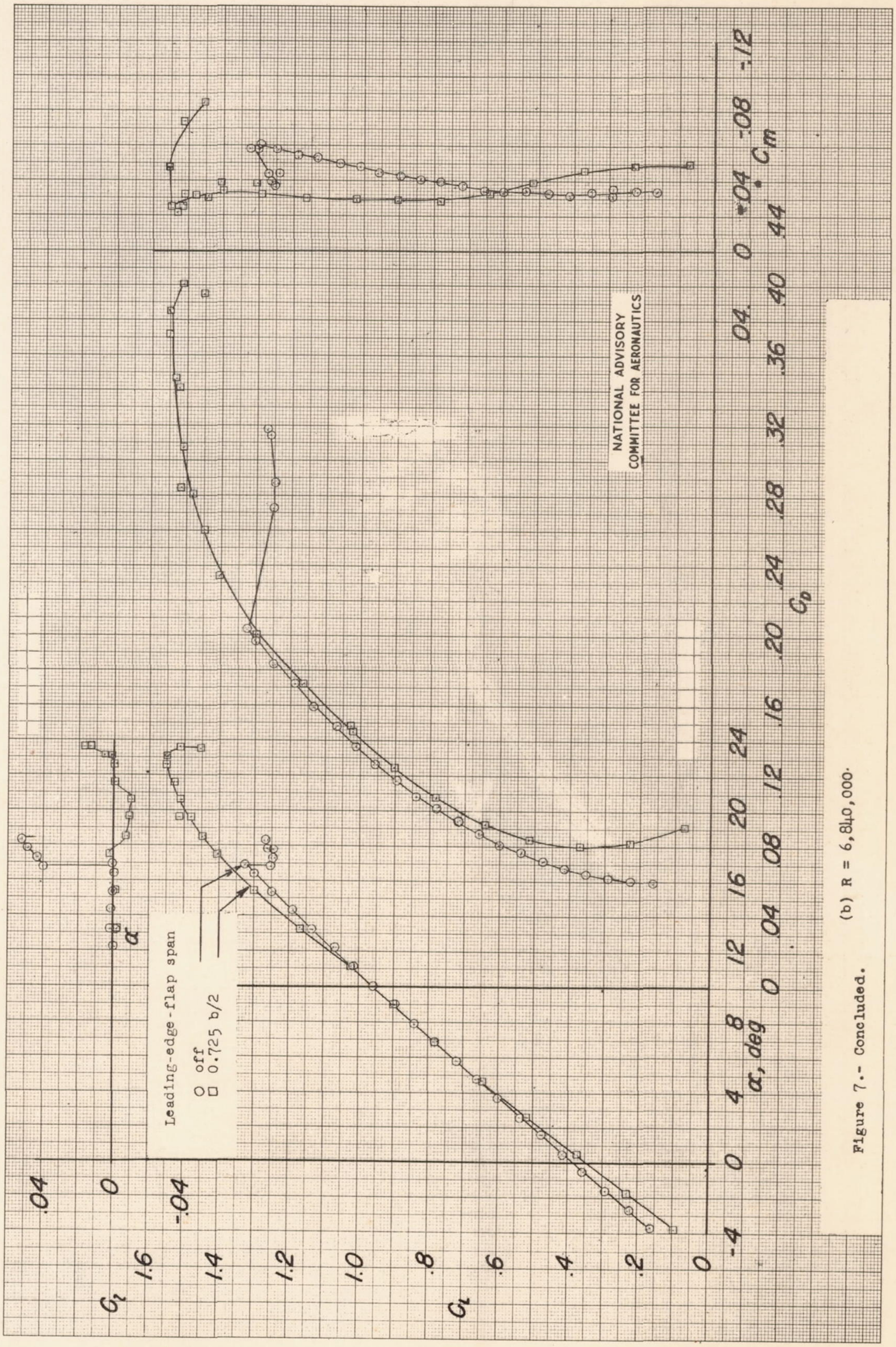

Figure 7.- Concluded. (b) R = 6,840,000.

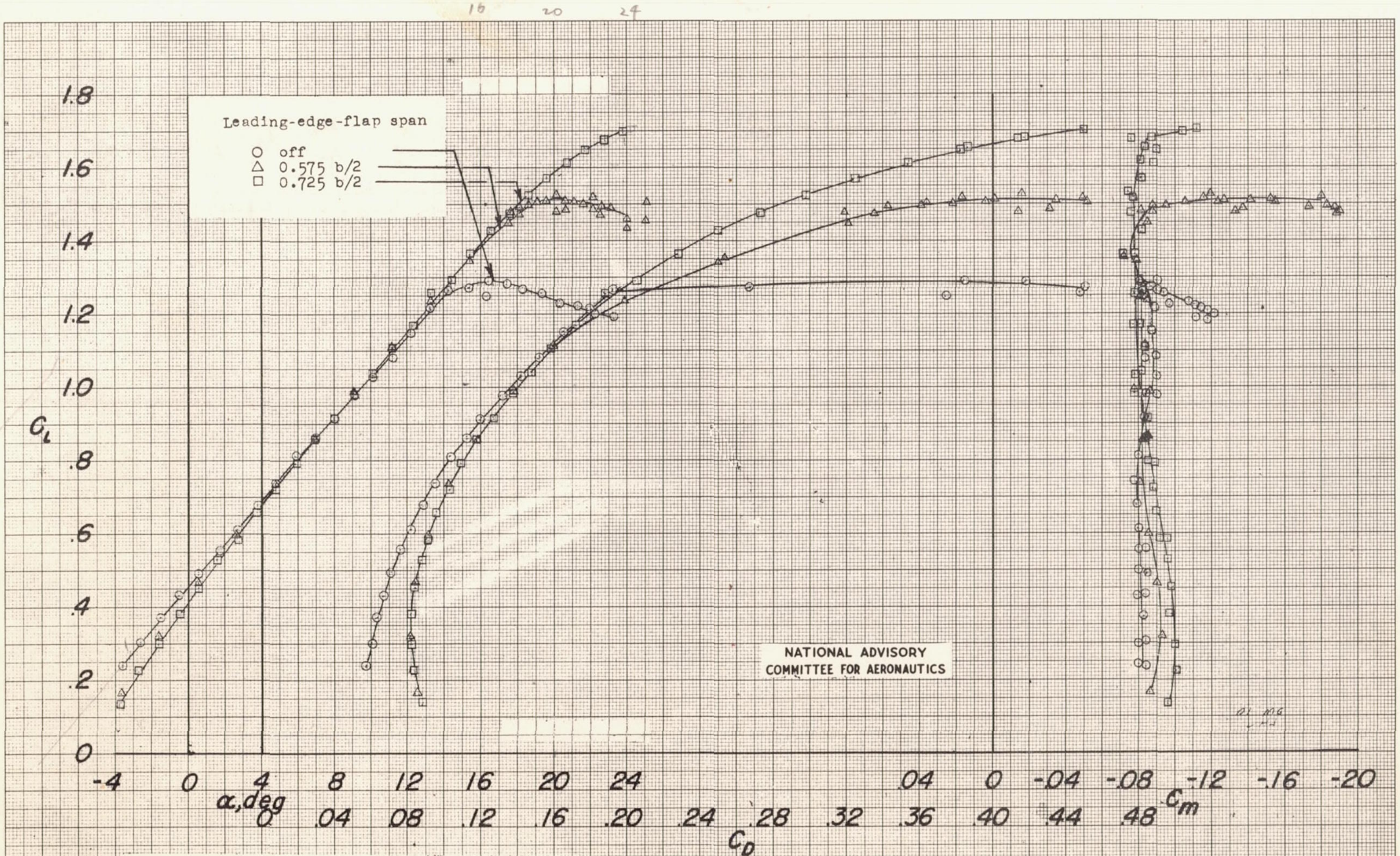

(a) R = 3,040,000.

Figure 8.- Aerodynamic characteristics of a 40° sweptback wing with and without leading-edge flaps. Extended split flaps on.

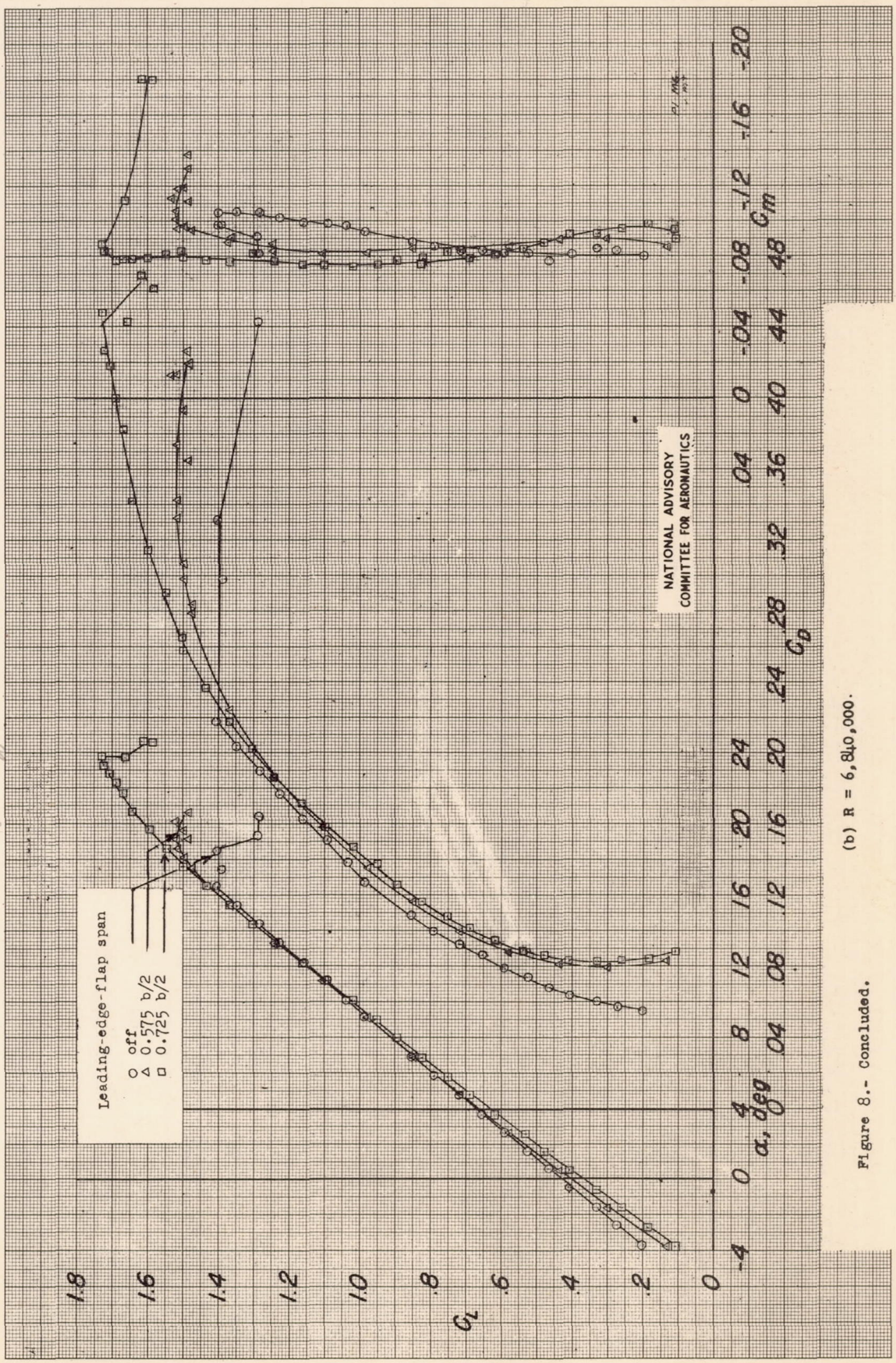

(b) R = 6,840,000.

Figure 8.- Concluded.

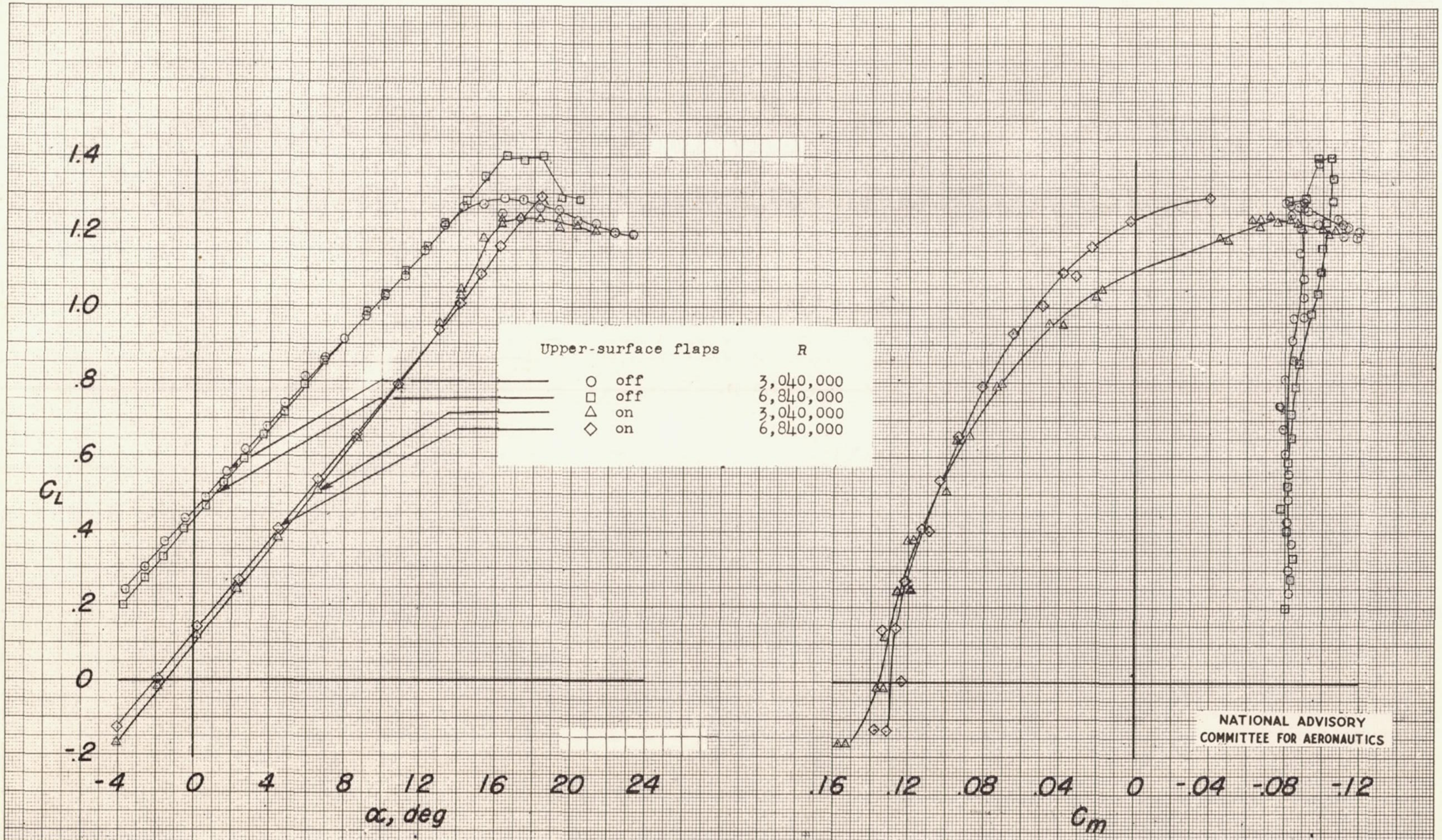

(a) C_L plotted against α and C_m.

Figure 9.- Aerodynamic characteristics of a 40° sweptback wing with and without upper-surface flaps. Extended split flaps on.

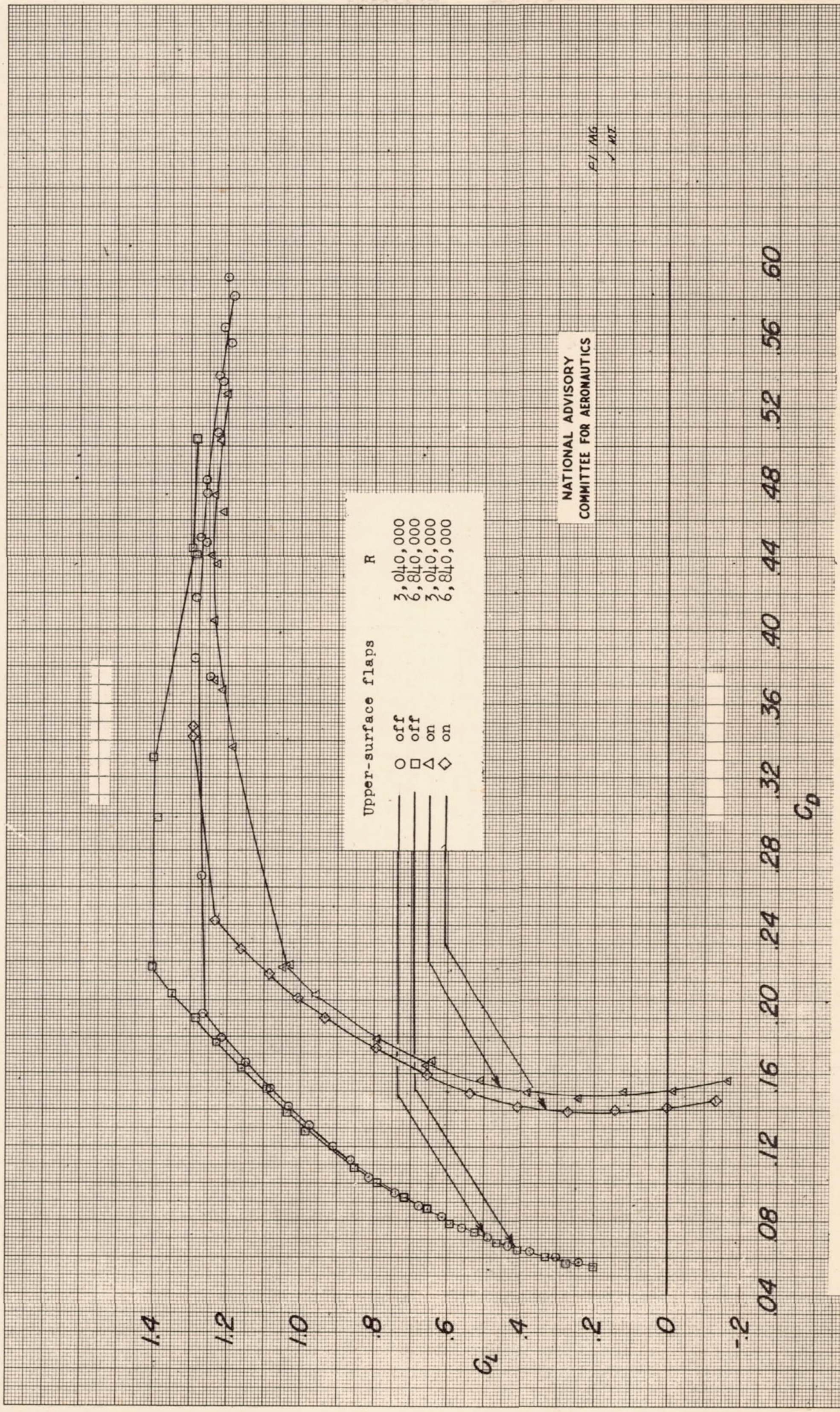

(b) C_L plotted against C_D.

Figure 9.- Concluded.

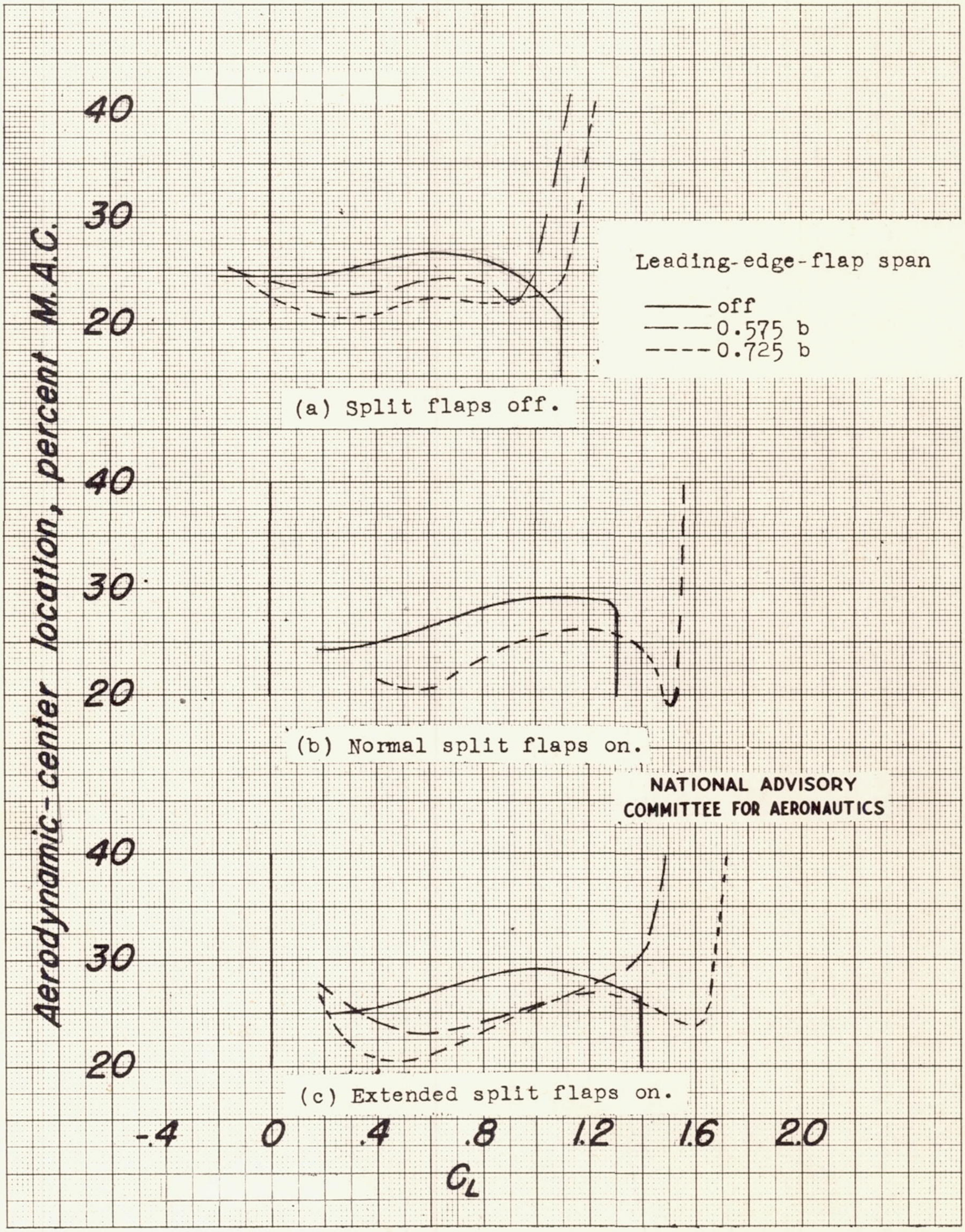

Figure 10.- Aerodynamic-center location for various leading-edge and trailing-edge flap combinations on a 40° swept-back wing. R = 6,840,000.

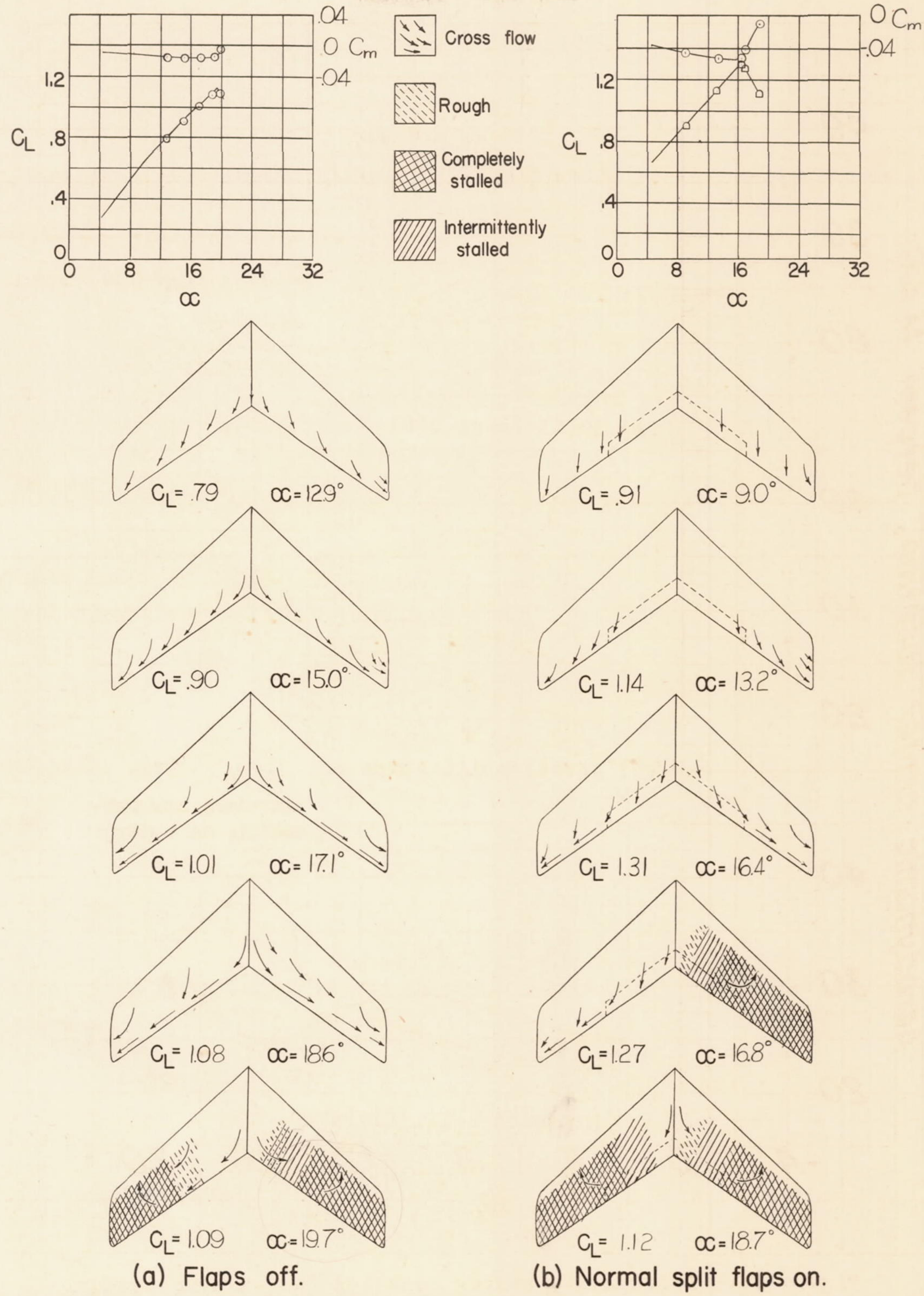

(a) Flaps off.

(b) Normal split flaps on.

Figure 11.- Stalling characteristics of 40° sweptback wing. R = 6,840,000.

NATIONAL ADVISORY COMMITTEE FOR AERONAUTICS

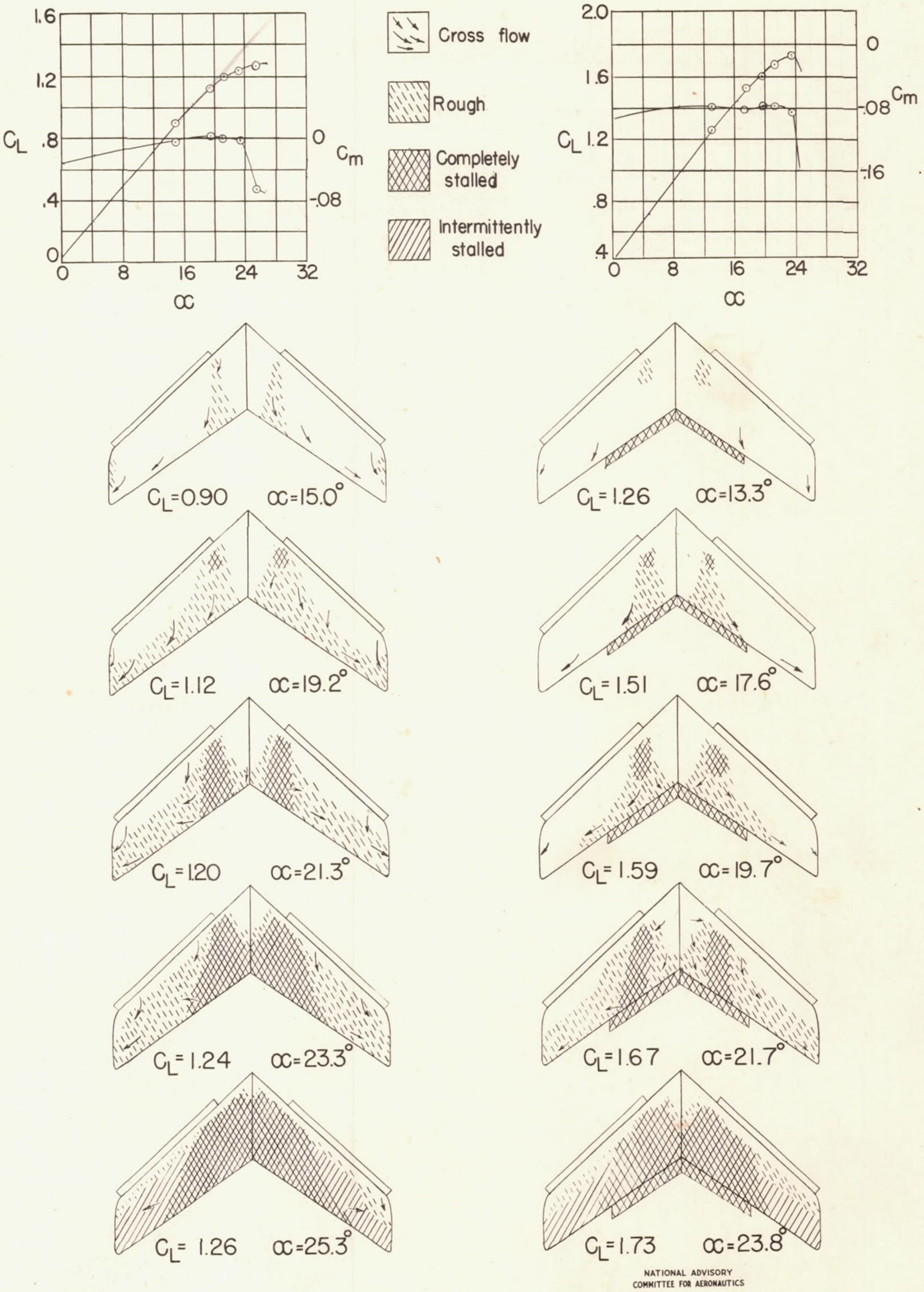

(a) 0.725 b/2 span leading-edge flaps on.

(b) 0.725 b/2 span leading-edge flaps and extended split flaps on.

Figure 12.- Stalling characteristics of a 40° sweptback wing with stall control flaps. R=6,840,000.

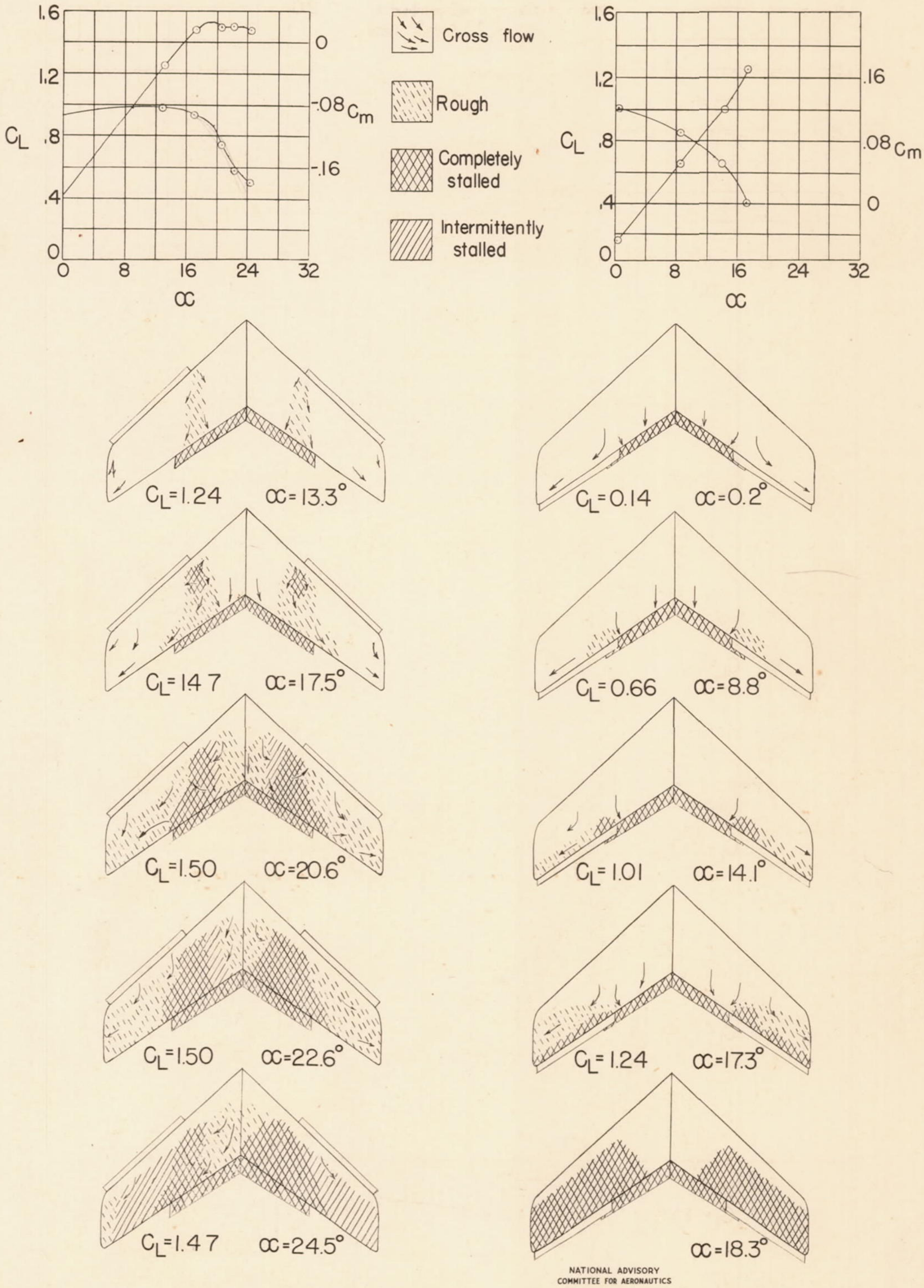

(c) 0.575 b/2 span leading-edge flaps and extended split flaps on.

(d) Upper-surface flaps and extended split flaps on.

Figure 12.- Concluded.

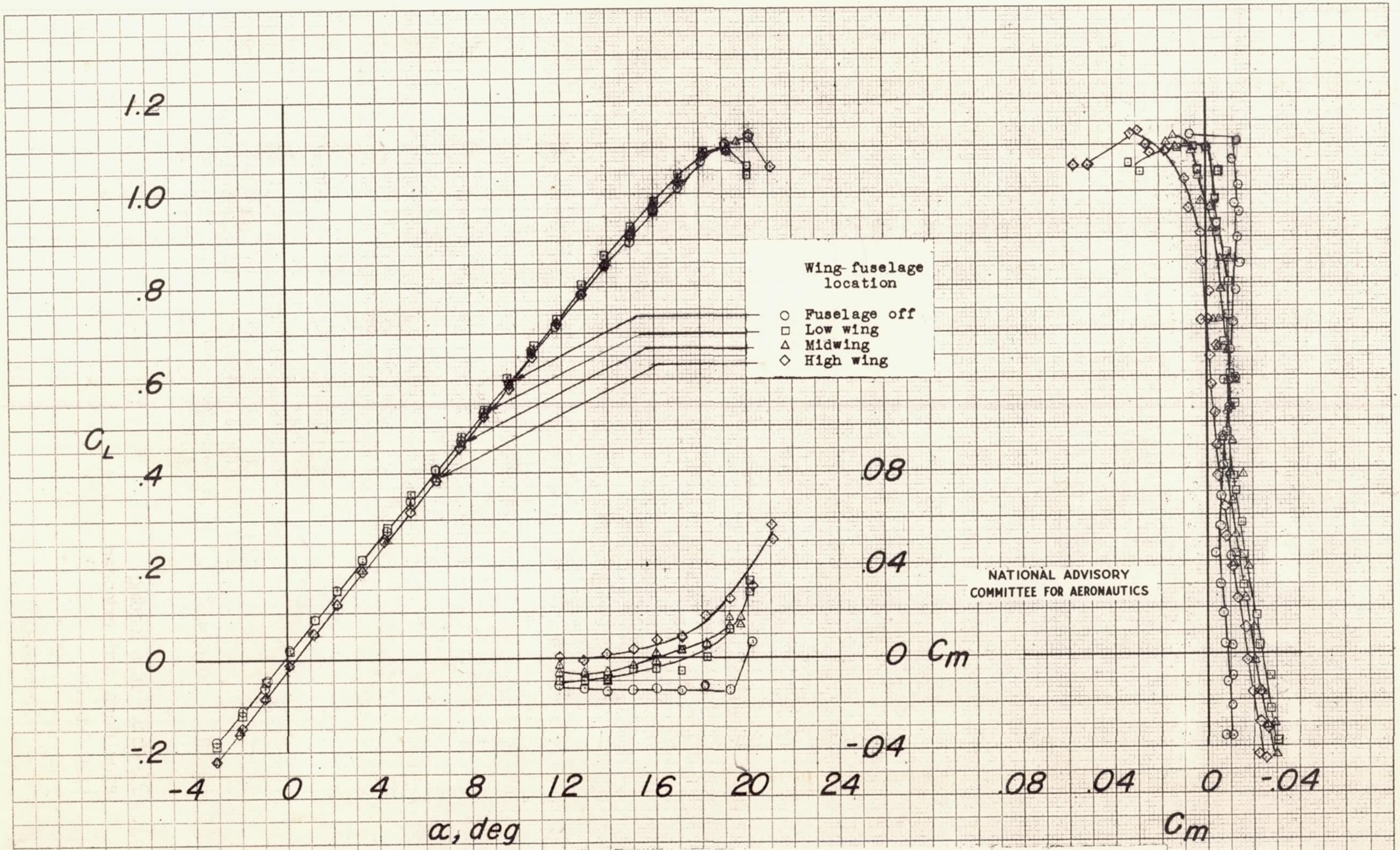

(a) C_L plotted against α and C_m.

Figure 13.- Aerodynamic characteristics of a 40° sweptback wing with fuselage on. Flaps off. R = 8,090,000.

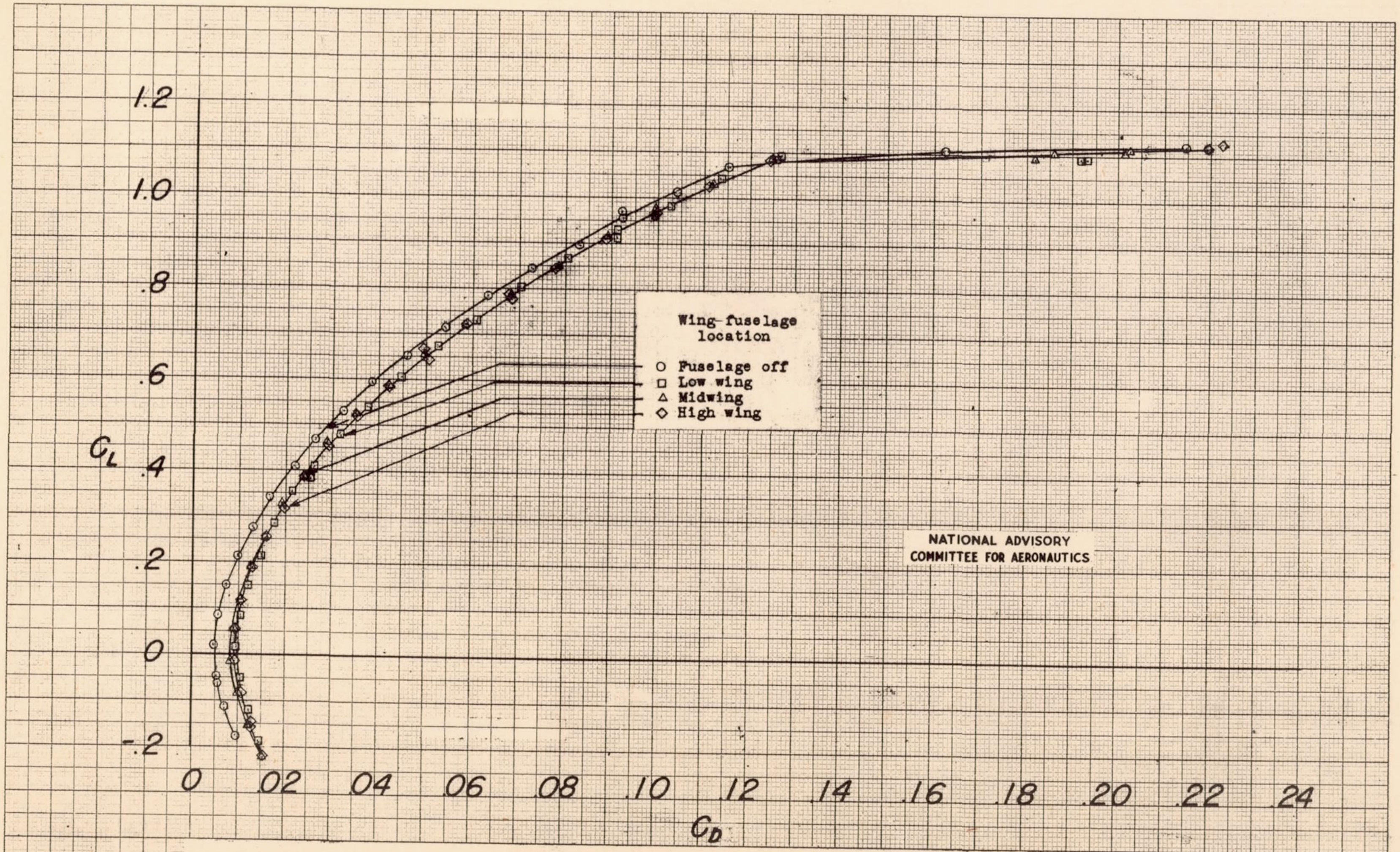

(b) C_L plotted against C_D.

Figure 13.- Concluded.

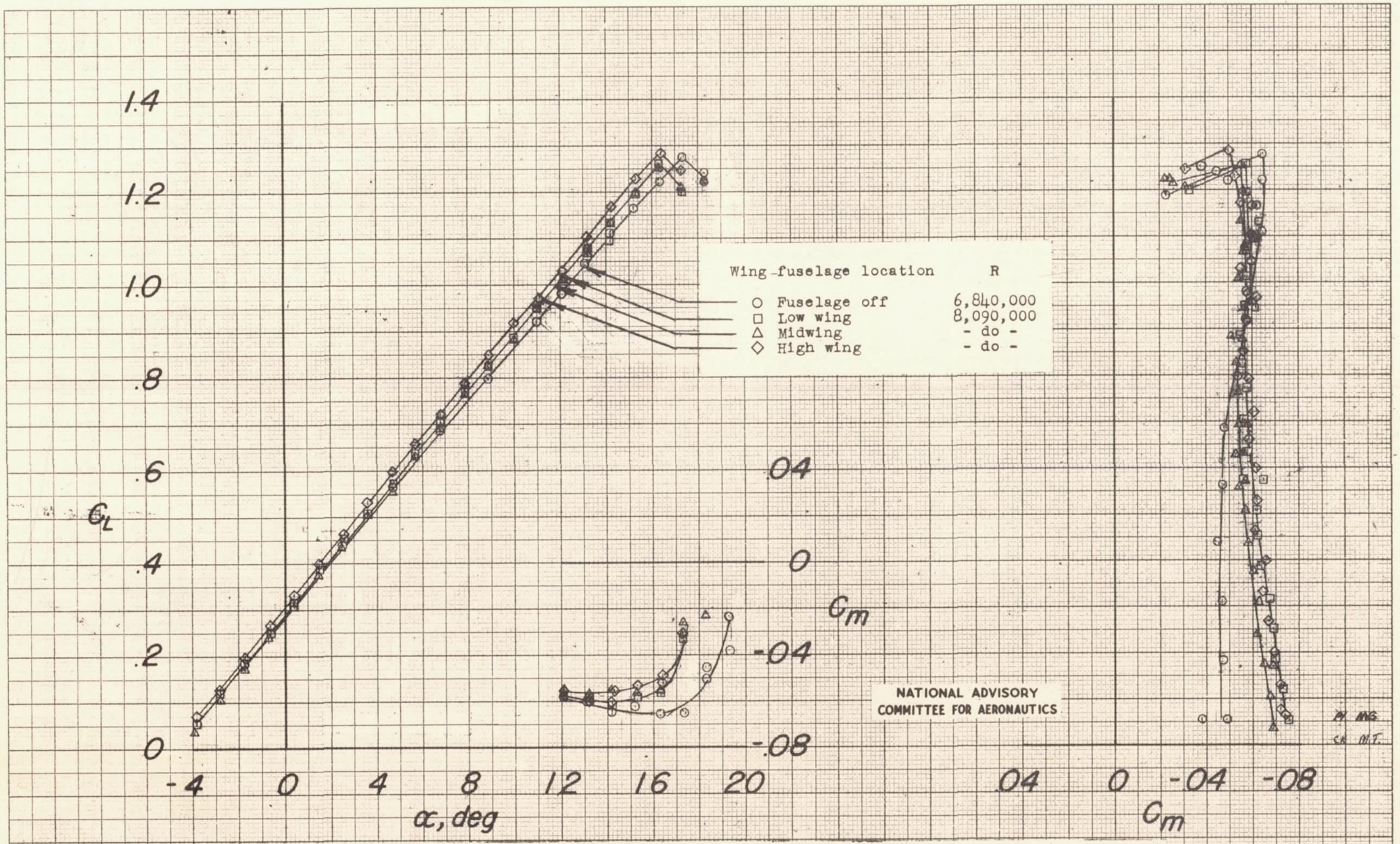

(a) C_L plotted against α and C_m.

Figure 14.- Aerodynamic characteristics of 40° sweptback wing with fuselage on. Normal split flaps on.

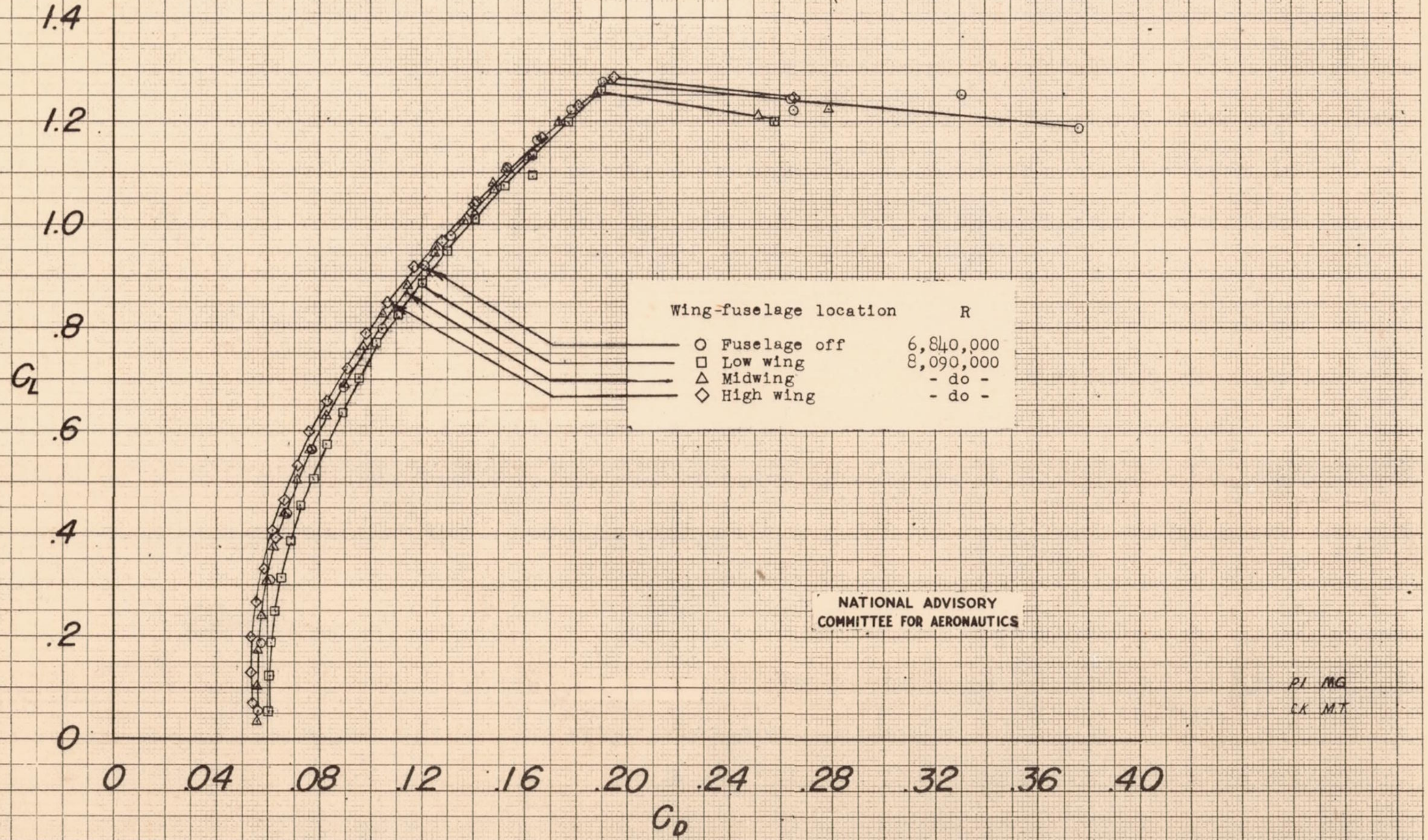

(b) C_L plotted against C_D.

Figure 14.- Concluded.

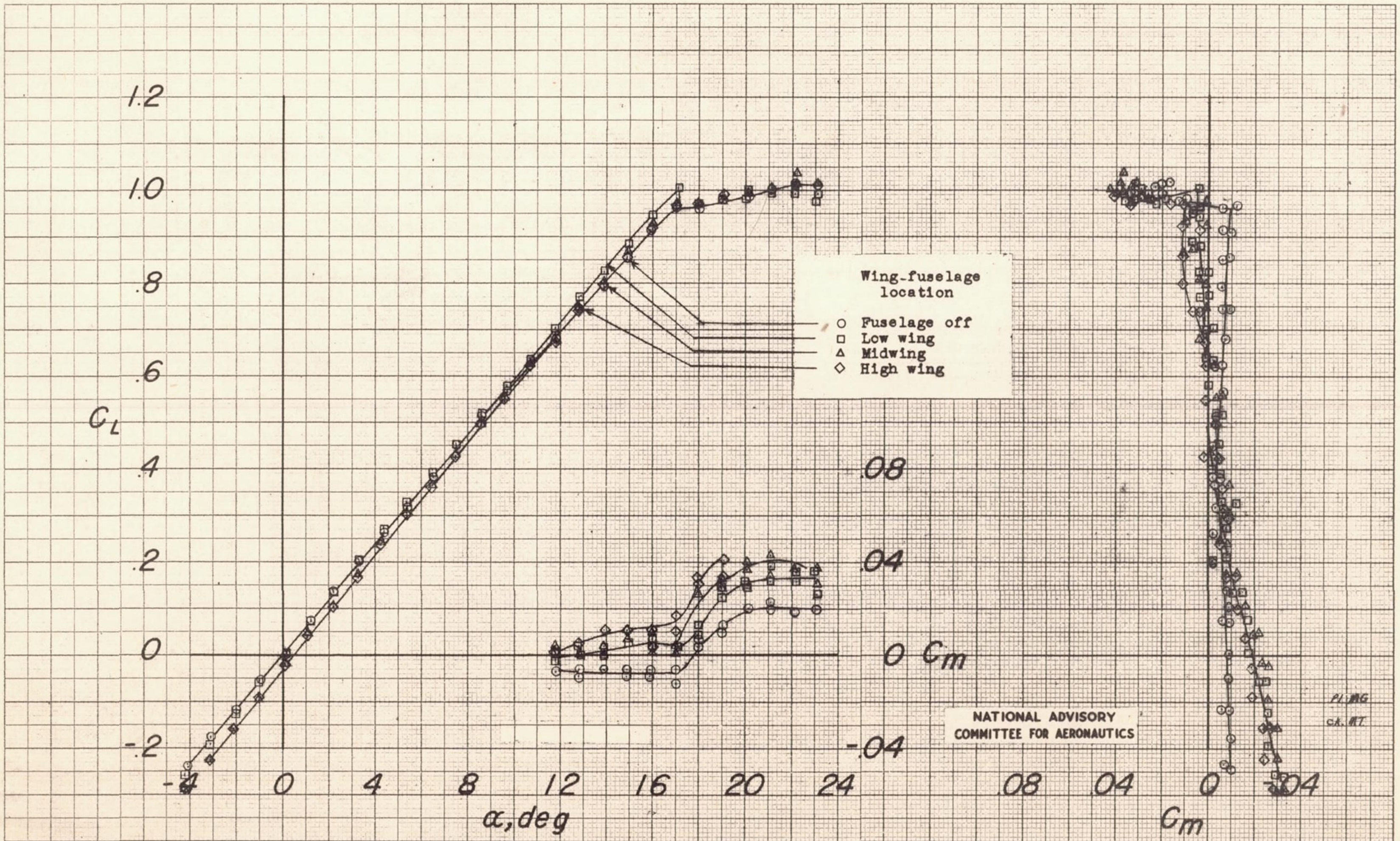

(a) C_L plotted against α and C_m.

Figure 15.- Aerodynamic characteristics of a 40° sweptback wing with fuselage on. Flaps off. R = 3,040,000.

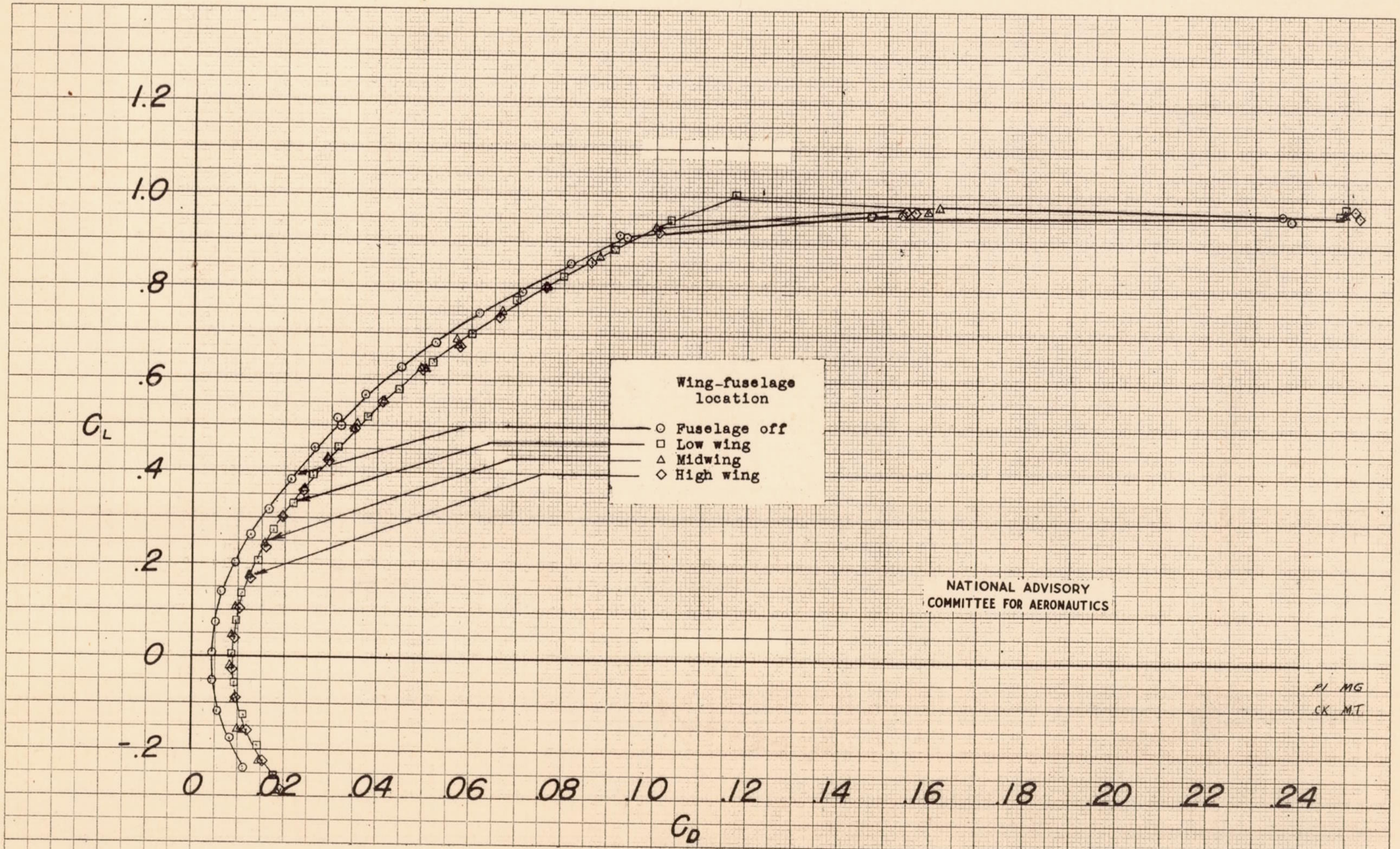

(b) C_L plotted against C_D.

Figure 15.- Concluded.

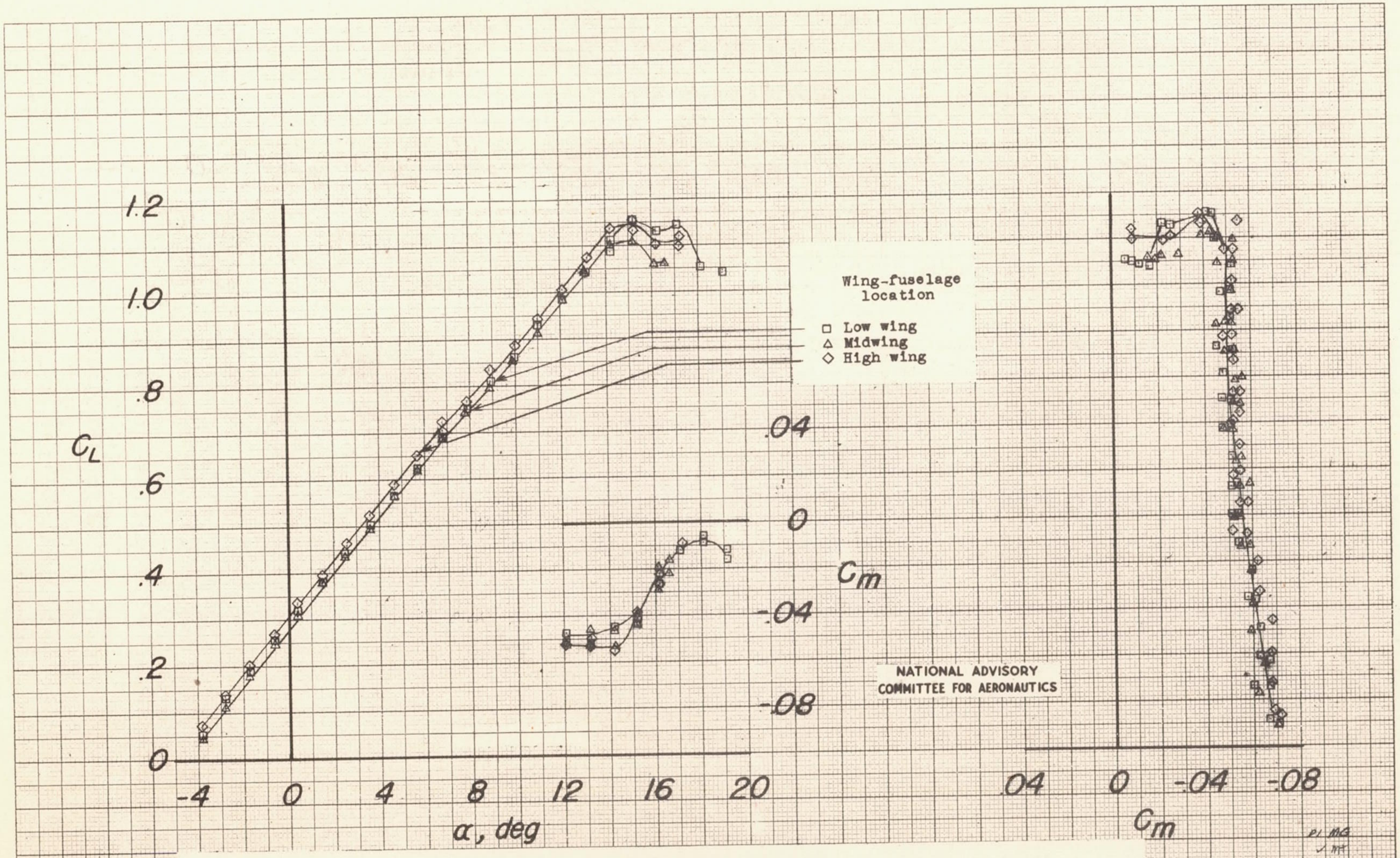

(a) C_L plotted against α and C_m.

Figure 16.- Aerodynamic characteristics of 40° sweptback wing with fuselage on. Normal split flaps on. R = 3,040,000.

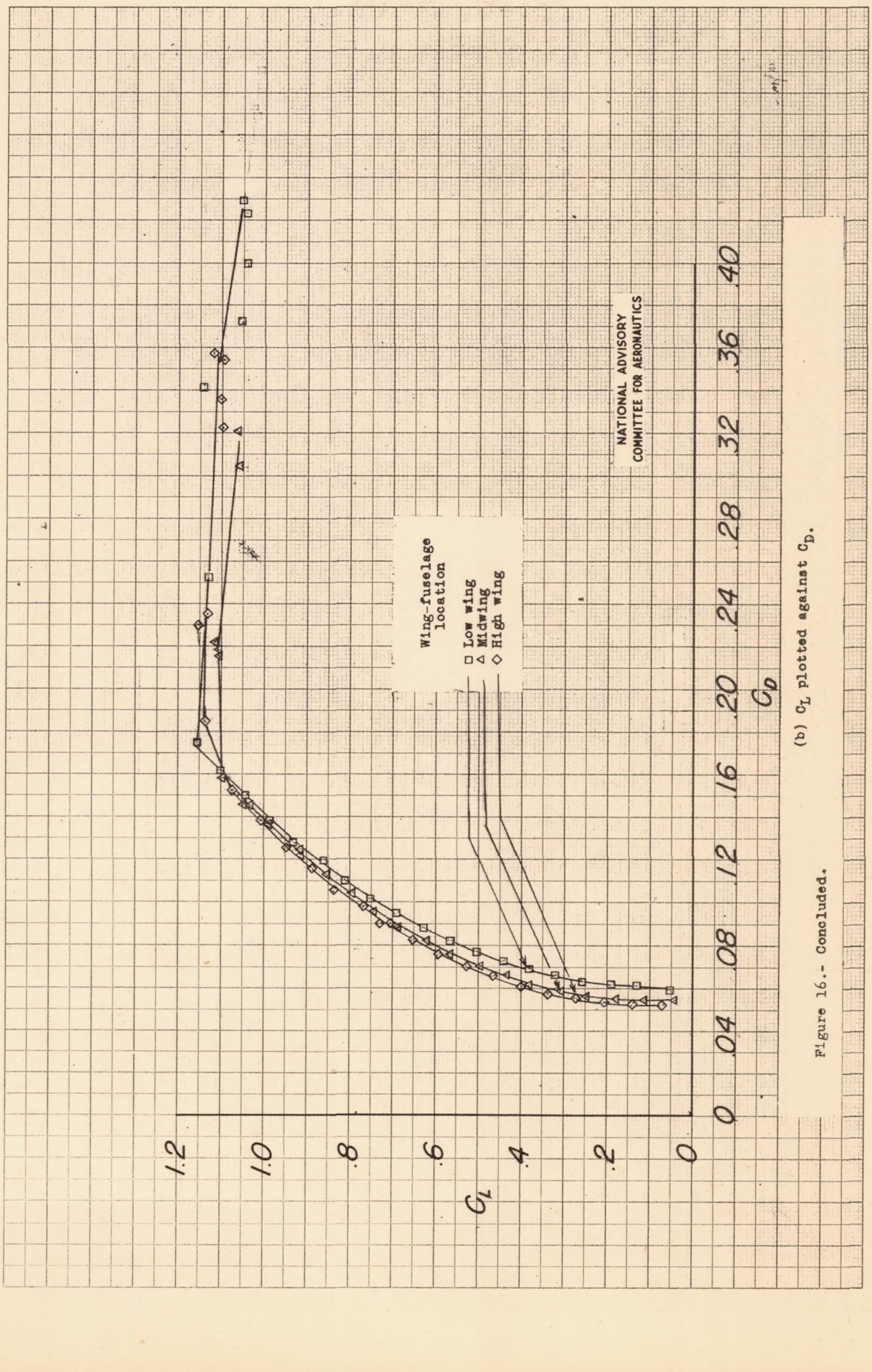

Figure 16.- Concluded.

(b) C_L plotted against C_D.

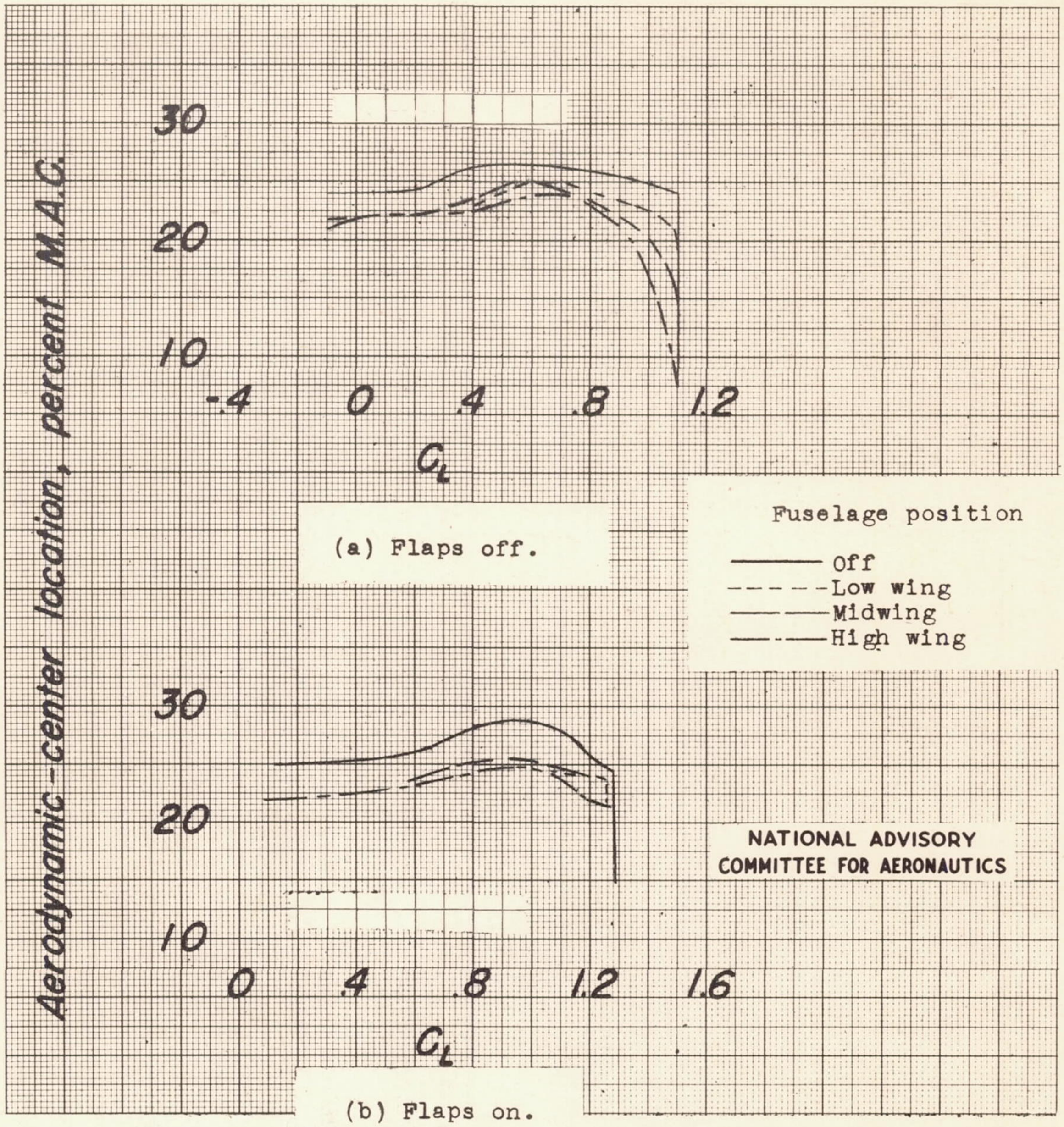

Figure 17.- Aerodynamic-center location for various positions of a fuselage on a 40° sweptback wing. R = 8,090,000.

115
92-95

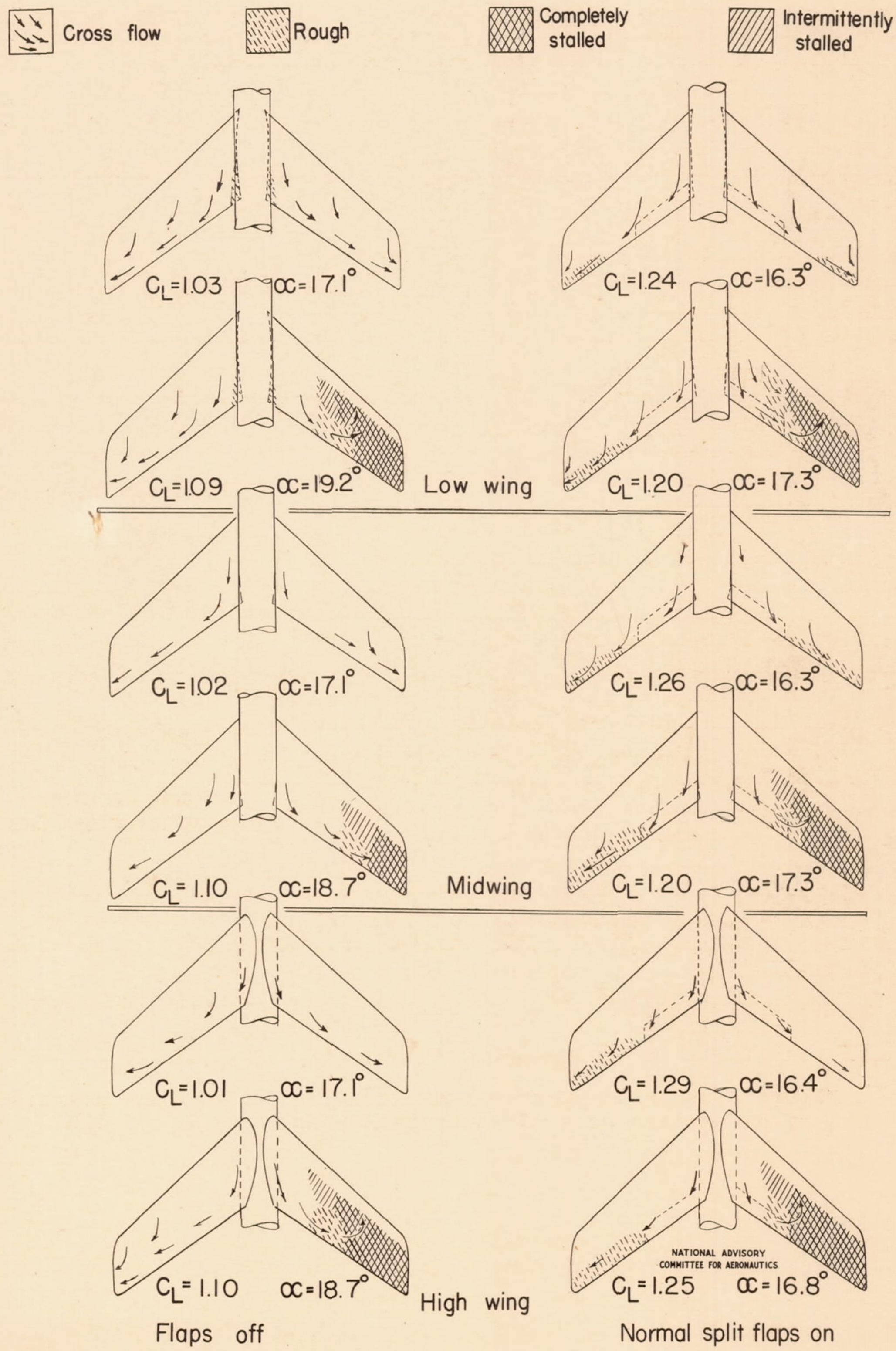

Figure 18.- Stalling characteristics of 40° sweptback wing with fuselage on. R = 8,090,000.